

FOREWORD

This report was prepared by Santa Rita Technology, Inc. for the 6570th Aerospace Medical Research Laboratories under Contract AF 33(657)-11331, Project No. 7233, "Biological Information Handling Systems and Their Functional Analogs," and Task No. 723301, "Biological Mechanisms for Signal Analysis." Some of the work was accomplished under earlier Contracts AF 33(616)-7800 and AF 33(657)-8016. The principal investigator for all of the work was Dr. John L. Stewart. A large part of the material reported herein was incorporated in University of Arizona Doctoral Dissertations by Dr. W. F. Caldwell and Dr. E. Glaesser, especially the latter who was the primary contributor to the outer-middle ear model. Contract monitors were Lt. V. E. Sackschewsky and Lt. Mark W. Cannon, Biophysics Laboratory, Biodynamics and Bionics Division.

We wish to thank members of the Biodynamics and Bionics Division for their continuing encouragement of our research. The task of building artificial equivalent animals is a long and difficult one that often demands the making of unconventional and even unpopular speculations. The acceptance of our particular approach to research by the Biodynamics and Bionics Division has been of basic importance to its success.

Contrails

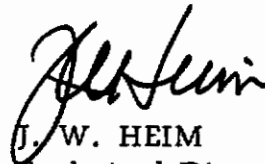
ABSTRACT

An electrical analog of the human ear is described, which includes the external and middle ear, the cochlea, and part of the neural structure of the cochlea and the higher auditory centers of the central nervous system. The analog is developed on the basis of a one-to-one relation between physiological and electrical parameters. The electrical analog cochlea is realized as a 36-section, lumped-parameter, nonuniform transmission line. The neural structure of the cochlea and auditory portions of the central nervous system are modeled functionally by means of 36 detecting and filtering amplifiers, termed loudness converters. The spatial array of the 36 loudness converter outputs is a neural-equivalent pattern of basilar membrane motion.

A pattern theory of loudness detection and sound recognition is discussed. On the basis of this theory, the analog ear exhibits a threshold of hearing curve which is approximately the same as that for a human. The important mechanical variable is found to be the velocity of the basilar membrane. The neural volley effect is included. Studies indicate that sound recognition with the analog is similar to that for a human.

PUBLICATION REVIEW

This technical documentary report has been reviewed and is approved.



J. W. HEIM
Technical Director
Biophysics Laboratory

INTRODUCTION	Page 1
STRUCTURE OF THE EAR	2
THEORY OF THE COCHLEA	6
The Cochlea	6
Equations of continuity	8
Equations of fluid motion	9
Equations of cochlear duct motion	9
Combined equations of motion	10
Electrical Analog of the Cochlea	10
Equations of the shunt branch	11
Equations of the series branches	11
Analog equations of correspondence	11
Sensory Loudness Conversion	14
PARAMETERS OF THE COCHLEA	16
Introduction	16
Dynamic Mass of the Cochlear Duct	17
Energy equivalent mass	17
Loading mass	19
Dynamic Friction of the Cochlear Duct	21
Dynamic Stiffness of the Cochlear Duct	21
Equivalent Friction of the Perilymph	23
DESIGN OF THE COCHLEA	24
Number of Sections	24
Impedance Scaling	24
Component Values	25
THEORY AND DESIGN OF THE OUTER AND MIDDLE EAR	25
Introduction	25
Development of the Analog	30
The outer ear	30
The tympanic membrane and the middle ear cavity	31
The ossicles and the cochlear windows	34
Other conduction paths and intratympanic reflexes	37
Practical Realization of the Analog	38
Simplification of the analog	38
Input impedances and transfer functions	38
DESIGN AND RESULTS	42
The Complete Analog Ear	42
Input Impedances	42
Velocity and Displacement of the Basilar Membrane	46
Loudness Phenomena	46
Sustained Sound Recognition	51
SUMMARY	54
APPENDIX	55
REFERENCES	66

LIST OF ILLUSTRATIONS

<u>Figure</u>		<u>Page</u>
1	Idealized Cross-section of the Ear	3
2	The Outer and Middle Ear	4
3	Cross section of the Cochlear Duct	5
4	Hydrodynamic Model of the Cochlea	7
5	Basic Cochlear Analog Section	12
6	Loudness Converter Block Diagram	15
7	Assumed Cross-section of the Cochlear Duct	18
8	Pattern Localization	22
9	Parallel and Series Branch Inductance	26
10	Series and Parallel Branch Resistance	27
11	C_p - Parallel Branch Capacitance	28
12	Block Diagram of the Outer and Middle Ear	29
13	Model of the Tympanic Membrane and the Middle Ear Cavity	32
14	Electrical Analog of the Tympanic Membrane and the Middle Ear Cavity	33
15	Model of the Ossicles and the Cochlear Windows	35
16	Electrical Analog of the Ossicles and the Cochlear Windows	36
17	Simplified Analog of the Outer and Middle Ear	39
18	Input Magnitude of the External Auditory Meatus	40
19	Input Impedance of the Middle Ear	41
20	Transfer Function Magnitude of the External Auditory Meatus	43
21	Transfer Functions of the Middle Ear	44
22	Block Diagram of the Ear	45
23	Input Impedance Phase and Magnitude of the Analog Cochlea	47

LIST OF ILLUSTRATIONS

<u>Figure</u>		<u>Page</u>
24	Circuit for Simulation of the Cochlea Input Impedance	48
25	Magnitude and Phase of Basilar Membrane Motion	49
26	Analog Threshold Curves for Velocity and Displacement	50
27	Comparison of Auditory Thresholds	52
28	Scatter Diagram - Cross Correlation Recognition	53
29	The Generalized Nodal System	57
30	Simplified Diagram of the Cochlea	57
31	Generalized System for Velocity	59
32	The First Order Equivalent for the Cochlea	59
33	The First Order Loop	60
34	The Second Order Nodal System	60
35	Equivalent Cochlea Based on Loop Current or Node Voltage Differences	62
36	Approximations for the Tympanic Membrane	64
37	The Second Order Approximation for the Tympanic Membrane	64

INTRODUCTION

The human hearing system constitutes a remarkable mechanism for the detection and recognition of sounds. It consists of the outer ear, the middle ear, the cochlea, and the associated regions of the central nervous system. It is the purpose of this report to describe research aimed at modeling this hearing system. The tools employed in the modeling are those commonly associated with modern communication and control theories.

A great deal of study has been devoted to hearing, both physiological and psychological (where psychological studies alone suffice when physiological procedures are not feasible, as in the living human). Only in recent years, however, have the definitive physiological investigations by Békésy given us the first real understanding of mechanisms underlying mechanical motions in the cochlea (ref. 1). Various attempts have been made to represent these motions with electric and hydraulic models (refs. 1-6).

Work reported here commenced in 1960 and has resulted in construction of two complete analogs, the first of which provided complete real-time patterns in 1961 (refs. 7-9). This effort is founded on a theory for hearing in which the functional nature of the conversion process between mechanical and neural variables figures importantly (refs. 10-12). The complete analog device shows many of the well-known phenomena in psychoacoustics (ref. 9). It has also been demonstrated that the analog recognizes vowels in a similar way to a human observer, and that the machine is relatively insensitive to the particular speaker and, for that matter, to whether the vowel is voiced or whispered (ref. 8). Also unique to the present analog is the relatively complete modeling of all three parts of the ear.

In the fall of 1962, the analog ear was employed for synthesizing speech. The results of this demonstrated beyond doubt that speech bandwidth compression to less than 20 cycles per second had been achieved. This result can be expected to lead to searching reappraisals of classical concepts in speech and hearing. Bandwidth compression requires first the accurate establishment of the transducing mechanism and secondly, the proper functional representation of what is believed to occur in the brain. Perhaps it is not purely accidental that bandwidth compression was virtually an automatic result of attempts to find the most complete representation for the human hearing system that was possible, using a combination of physiological and psychological data with speculation and notions of optimum detection theories.

Many of the ideas for signal processing were developed in mid 1960, especially detection concepts. These ideas were spread rather widely through personal communications and proposals for research support. Support was acquired, and the first complete system for displaying patterns was operated in the fall of 1961. It is believed that this was the first such system in reasonably complete form. The general description for the design of the analog and a fairly extensive treatment of detection concepts (including part of the bandwidth compression methodology) were presented orally in the fall of 1961 at the Bionics Symposium, with corresponding papers published in 1962 (refs. 7,10). The oral presentation was just before the analog operated for the first time; earlier predictions and theoretical concepts proved to be accurate.

The approach to construction of a one-to-one electrical analog starts with an idealized model for the cochlea for which dynamical equations are written. The electrical analog is found which obeys the same equations. Necessary parameters are evaluated from experimental data. A similar procedure is followed for outer and middle parts of the ear. The mechanism of the sensory elements of the ear is functionally simulated so as to provide a loudness converted pattern of neural excitation along the cochlea.

An explanation for sound recognition and psychoacoustic phenomena may be based on a pattern theory of general sensory stimulus recognition. The dynamic physical parameters of the cochlea are such that the energy associated with different frequencies tends to localize at different points along the cochlea, high frequencies near the stapes and low frequencies near the helicotrema.* Sensory structures convert mechanical energy into a monopolar spatial pattern of loudness along the cochlear duct. The pattern theory hypothesizes that sounds are recognized by the shape of this spatial pattern of loudness, where a short time average (order of a small fraction of a second) smoothes over a number of cycles of the stimulus frequency (and also over a number of adjacent neural pulses). The recognition of time varying sounds, such as speech, thus corresponds to the recognition of a three-dimensional surface of loudness in space and time.

STRUCTURE OF THE EAR

The general structure of the ear is shown in idealized cross-section in figure 1. The ear may be divided into three parts: the outer ear, the middle ear, and the inner ear. The outer ear consists of the pinna and the external auditory meatus, which is a tube closed by the tympanic membrane. The middle ear is made up of the tympanic membrane, an air-filled cavity, and the ossicular chain (malleus, incus, and stapes) which is contained within the cavity. The outer and middle ear serve to transmit sound to the inner ear. The outer and middle ear are shown in figure 2.

The inner ear consists of two units: the semicircular canals which serve to sense gravitational orientation and motion, and the cochlea which functions as a sound analyzing detector. The cochlear cavity is coupled to the middle ear by two flexible membrane-covered openings, or windows, in the bone. The stapes is attached to the membrane of the oval window such that a force on the stapes is transmitted into the fluid facing the oval window.

The cochlea consists of a snail-shaped cavity of about $2 \frac{3}{4}$ turns lying within the temporal bone, as illustrated in figure 1. The cavity has its largest area and radius of curvature at the basal end. It is divided into two channels, the scala vestibuli and the scala tympani, by a flexible triangular partition, the cochlear duct, illustrated in cross-section in figure 3. This partition extends from the basal to the apical end of the cochlea, at which point there is a small opening between the scalae, the helicotrema.

* Although localization appears at first glance to be into bands as in a spectrum analyzer, it is emphasized that phenomena of major importance arise because of an unsymmetric and continuous band overlap.

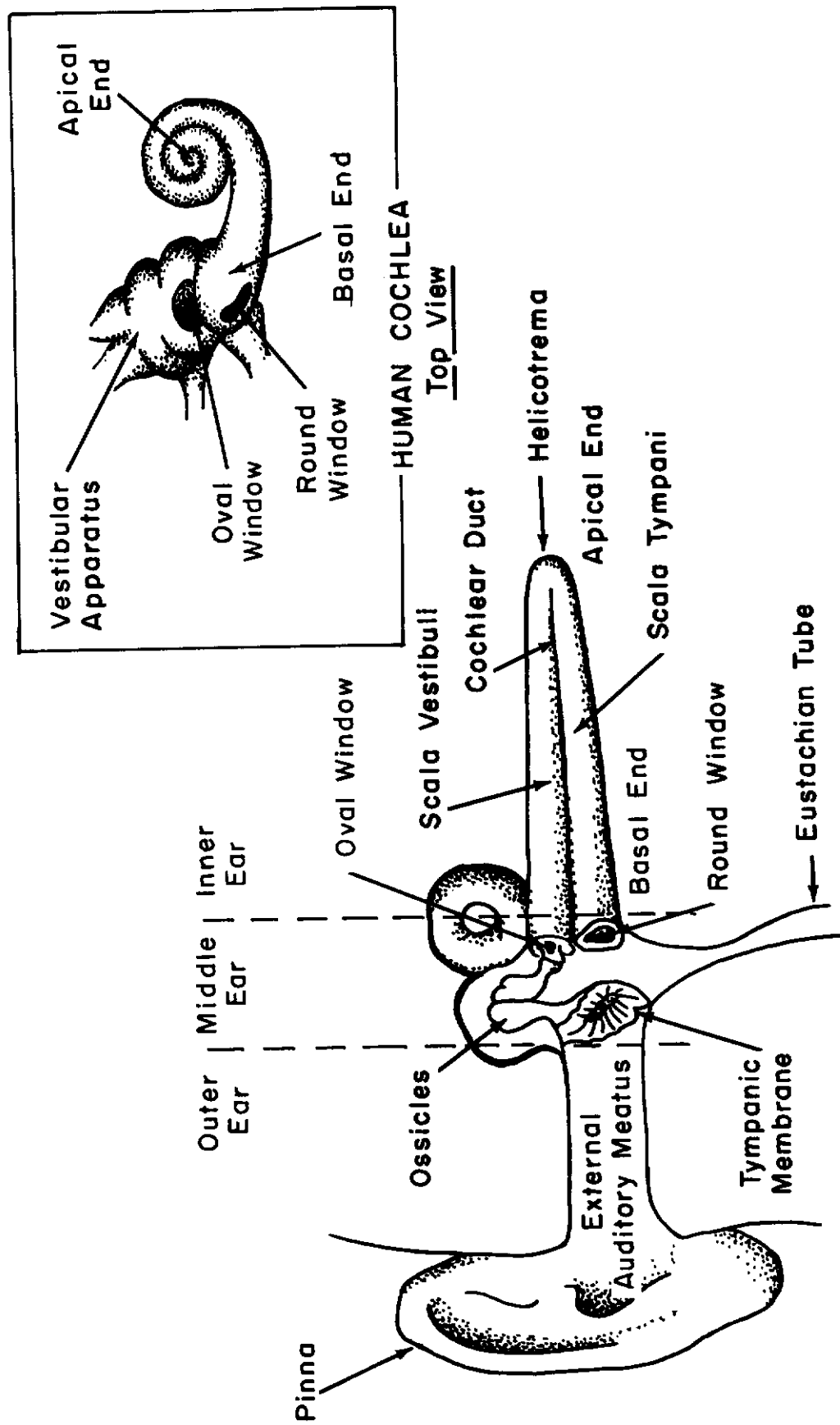


Figure 1. Idealized Cross-section of the Ear

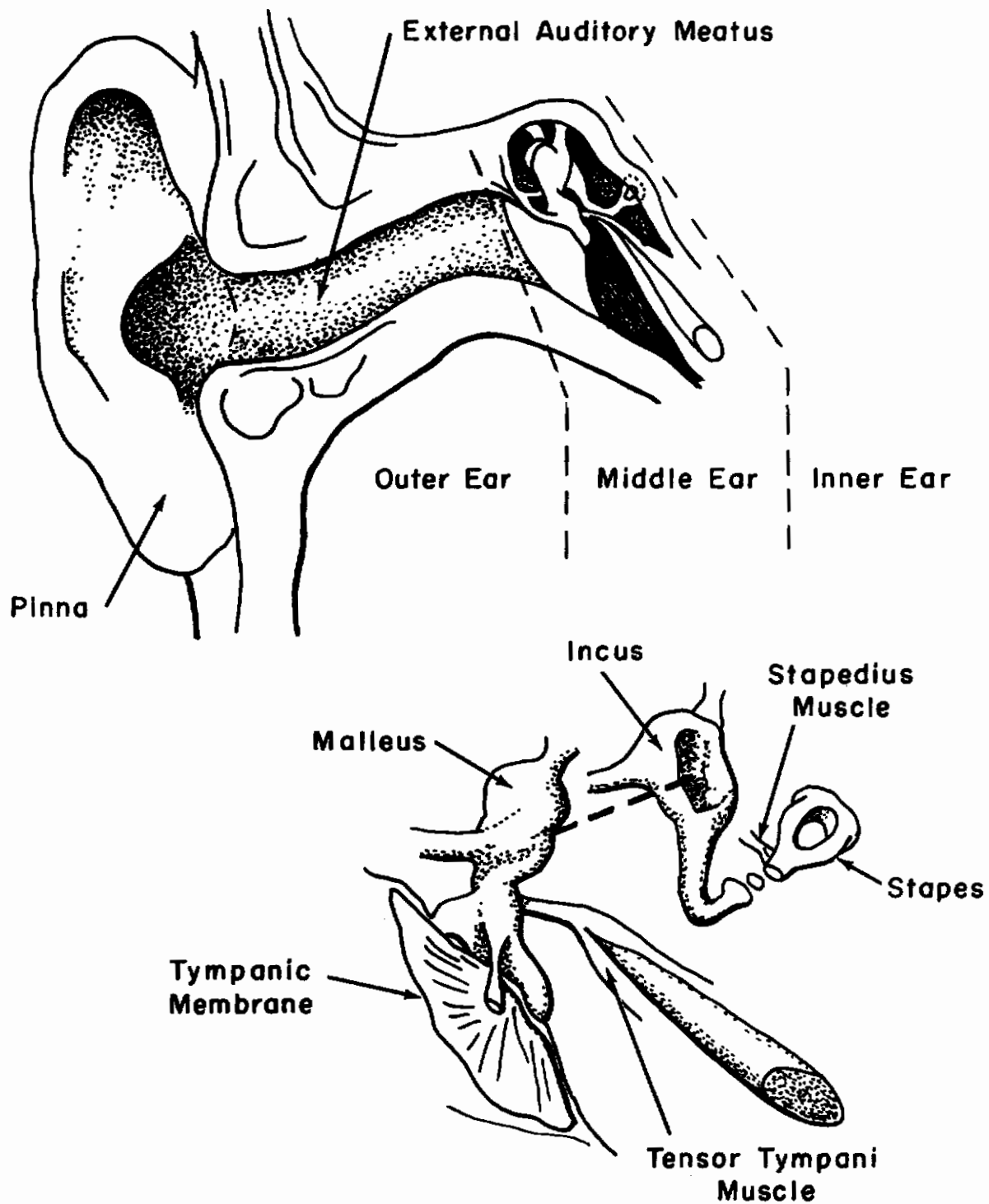


Figure 2. The Outer and Middle Ear

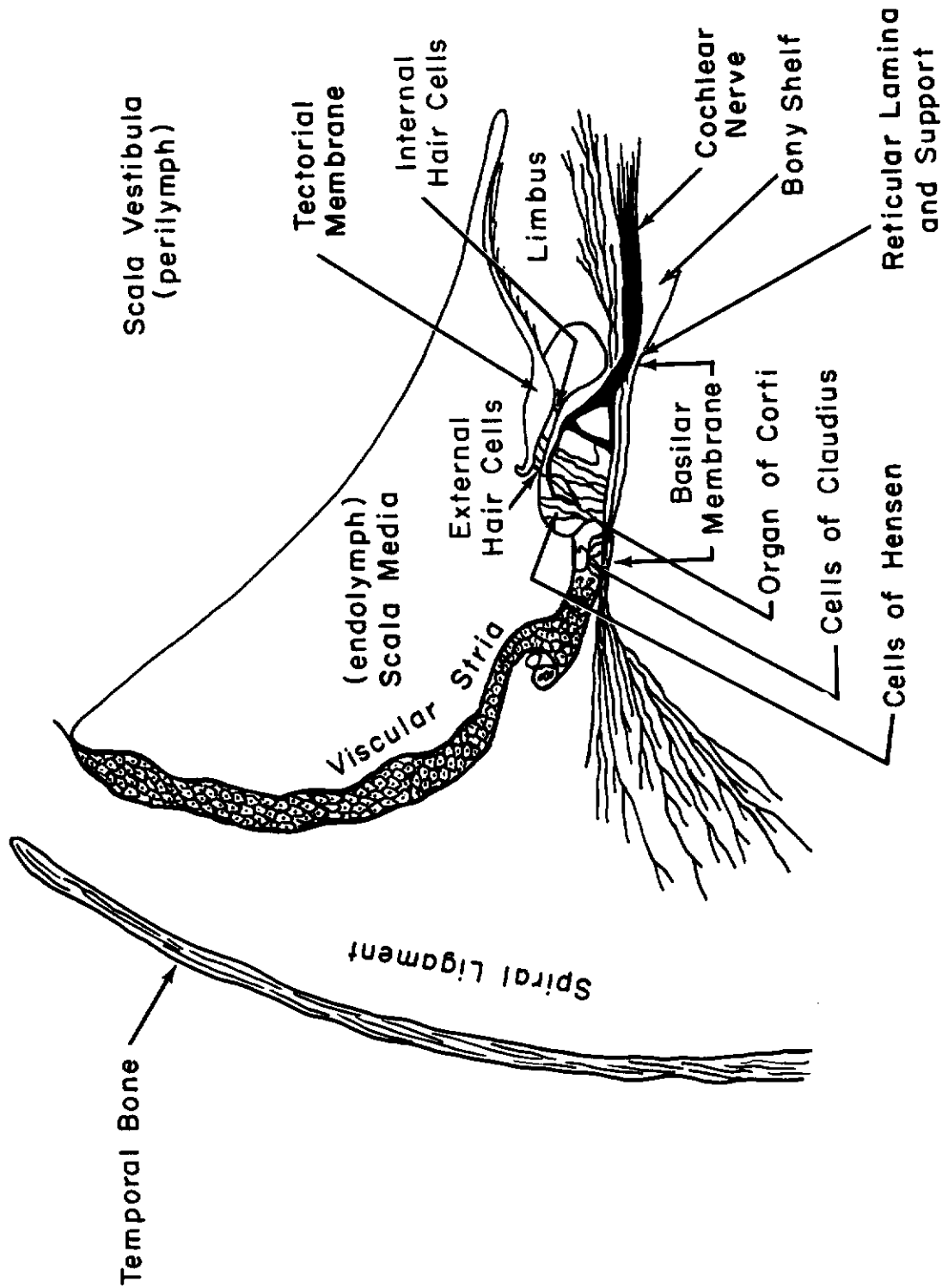


Figure 3. Cross section of the Cochlear Duct

Contrails

The scala vestibuli and the scala tympani are filled with perilymph, a fluid having a density about that of water and a coefficient of viscosity about twice that of water. The cochlear duct contains a viscous fluid, endolymph, and sensory elements. Reissner's membrane is thin and very flexible, while the basilar membrane is a fibrous elastic membrane upon which lies the sensory structure of the cochlea. The sensory structure is composed mainly of supporting cells, sensory cells, and nerve endings. This structure, the organ of Corti, contains about 20,000 hair cells with each cell containing four or five hairlike structures, the cilia. One end of each cilium extends through the scala media and is embedded into the tectorial membrane. Nerve fibers innervate the hair cells and pass, as the auditory nerve, to higher auditory centers of the central nervous system. As the basilar membrane bulges upward or downward, a shearing action of the cilia is created which causes neural excitation. The end result of a sound is thus a pattern of neural excitation in the auditory cortex of the brain. It is assumed that, when neural pulses from any particular segment of the cochlea reach the higher centers of the central nervous system, the pulses occur in such profusion as to be adequately represented by a continuous waveform; this assumption constitutes an important part of the pattern theory.*

THEORY OF THE COCHLEA

The Cochlea

The hypothesized model of the cochlea is shown in figure 4. It is assumed to be an idealized small signal cochlea in which nonlinearities are ignored. From this model the partial differential equations of continuity and of motion are written to describe pressure and velocity distributions in the cochlea. The basic assumptions are:

1. The perilymph is an incompressible fluid.
2. The walls of the cochlea are rigid.
3. The cochlear duct consists of independent elements of length Δx , each with mass, elasticity, and friction.
4. The distension of each element of the cochlear duct is parabolic.

Based on these assumptions, the dynamics of the cochlea are expressed by the following equations:

1. Equation of fluid continuity in the two scalae.
2. Equation of fluid motion in the two scalae.

* An analogy is to electron flow in a vacuum tube. Although individual electrons must be described in terms of short pulses of charge flow, the over-all average effect may be interpreted in terms of a continuous flow. A philosophy like statistical mechanics may be more fruitful for modeling macroscopic human processes than the neurone approach.

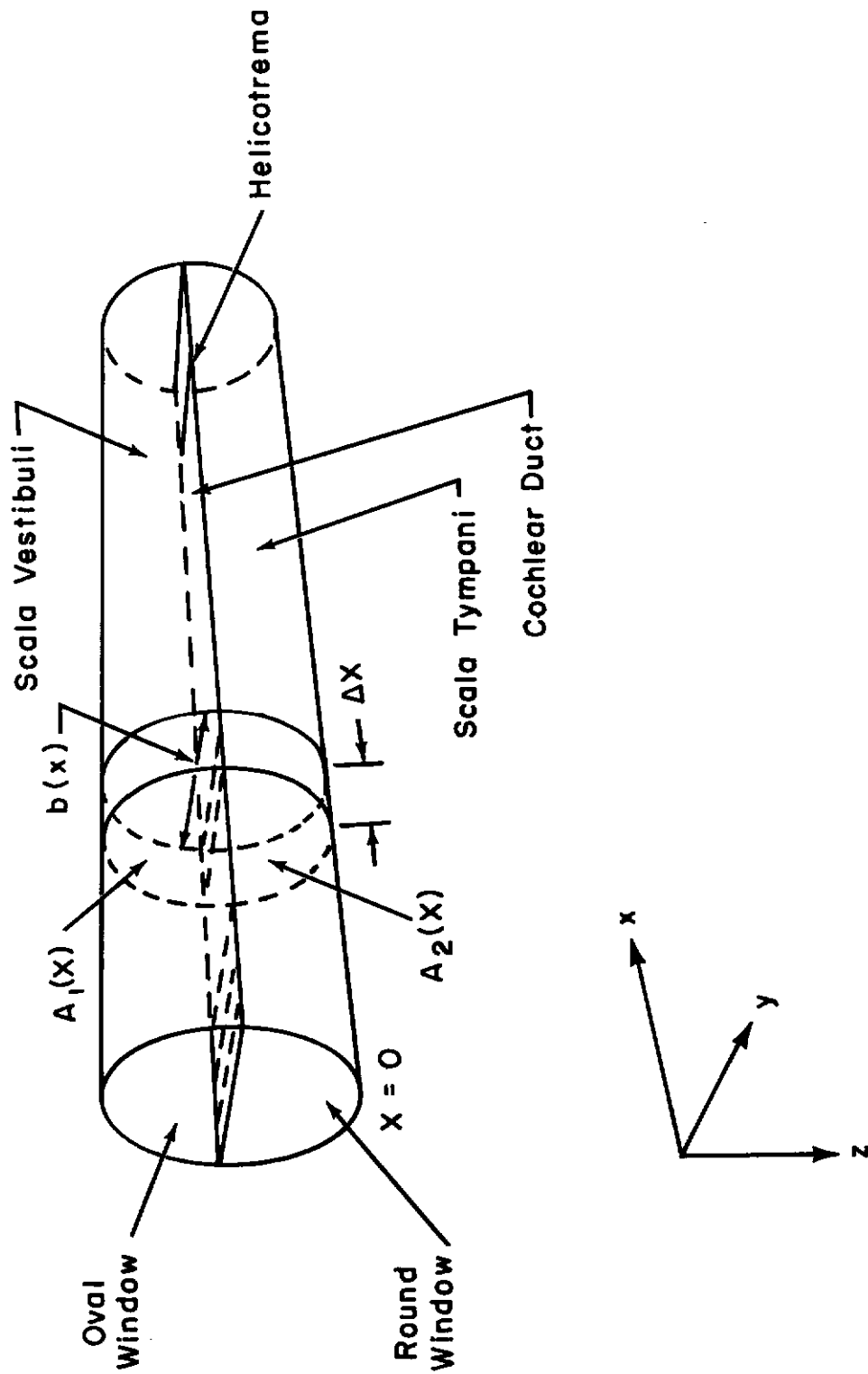


Figure 4. Hydrodynamic Model of the Cochlea

3. Equation of motion of an element of the cochlear duct.

It is pointed out that several investigators have proposed general hydrodynamic equations for the cochlea, although differences in mathematical approach do exist (refs. 2,3,4). The present analysis yields a unique set of element values with correspondingly different analog measures for cochlear patterns of mechanical activity. It is pointed out that the final analog network is a first-order approximation for almost any physical phenomenon explainable in terms of sets of linear differential equations. The network structure is hardly unique; it is the system of element values that characterizes the validity and accuracy of the result.

To proceed with the mathematical development, it is necessary to define the following parameters:

1. $A_1(x)$: Area of the scala vestibuli.
 $A_2(x)$: Area of the scala tympani.
 $A(x)$: Area of the scalae under the assumption of equal areas.
2. x, y, z : Coordinates for the righthand coordinate system shown in figure 4. When used for subscripts, the letter coordinate is indicated.
3. u_x, u_y, u_z : Velocity components in the x, y, z coordinates, respectively.
4. $b(x)$: Width of the basilar membrane.
5. $p(x, t)$: Sound pressure, a function of distance and time.
6. $m(x)$: Equivalent dynamic mass per unit length of the cochlear duct.
7. $f(x)$: Equivalent dynamic friction per unit length of cochlear duct.
8. $k(x)$: Equivalent dynamic stiffness per unit length of cochlear duct.
9. ρ_p : Density of the perilymph.
10. $f_p(x)$: Equivalent friction of the perilymph per unit volume of the scala.
11. $F(x, t)$: Force, a function of distance and time.

Subscripts 1 and 2 refer to the scala vestibuli and the scala tympani, respectively.

Equations of continuity. Under the assumption that the perilymph is incompressible, the equation of continuity for the scala vestibuli is:

$$\frac{d(\text{volume})}{dt} = 0 = u_{x1}(x,t)A_1(x) - u_{x1}(x+\Delta x,t)A_1(x+\Delta x) - \frac{2}{3}b(x)\Delta x u_z(x,t) \quad (1)$$

The coefficient of the last term, $2/3$, is the result of the assumed parabolic distension of the element representing the cochlear duct.

For Δx small:

$$u_{x1}(x+\Delta x,t) = u_{x1}(x,t) + \frac{\partial u_{x1}(x,t)}{\partial x} \Delta x \quad (2)$$

and

$$A_1(x+\Delta x) = A_1(x) + \frac{\partial A_1(x)}{\partial x} \Delta x \quad (3)$$

Thus, the equation of continuity in the scala vestibuli is:

$$0 = - \frac{\partial}{\partial x} [u_{x1}(x,t)A_1(x)] - \frac{2}{3}b(x)u_z(x,t) \quad (4)$$

and similarly, the equation for continuity in the scala tympani is:

$$0 = - \frac{\partial}{\partial x} [u_{x2}(x,t)A_2(x)] + \frac{2}{3}b(x)u_z(x,t) \quad (5)$$

These equations for the two scalae may be written to express the conditions of continuity in the cochlea as:

$$u_z(x,t) = - \frac{3}{2} \frac{1}{b(x)} \frac{\partial}{\partial x} [u_{x1}(x,t)A_1(x)] \quad (6)$$

$$u_z(x,t) = \frac{3}{2} \frac{1}{b(x)} \frac{\partial}{\partial x} [u_{x2}(x,t)A_2(x)] \quad (7)$$

Equations of fluid motion. To obtain the equations of fluid motion, it is assumed that the flow of fluid is negligible in all directions except along the axis of the cochlear scala. The force across a fluid element of the scala vestibuli is:

$$\Delta F_{x1}(x,t) = F_{x1}(x,t) - F_{x1}(x+\Delta x,t) = \left[f_p(x) \frac{\partial x_1(x,t)}{\partial t} + \rho_p \frac{\partial^2 x_1(x,t)}{\partial t^2} \right] A_1(x) \Delta x \quad (8)$$

This may be expressed in terms of pressure per unit length and fluid velocity as:

$$\frac{\Delta P_1(x,t)}{\Delta x} = \frac{f_p(x)}{A_1(x)} [u_{x1}(x,t)A_1(x)] + \frac{\rho_p}{A_1(x)} \frac{\partial}{\partial t} [u_{x1}(x,t)A_1(x)] \quad (9)$$

and similarly for the scala tympani:

$$\frac{\Delta P_2(x,t)}{\Delta x} = \frac{f_p(x)}{A_2(x)} [u_{x2}(x,t)A_2(x)] + \frac{\rho_p}{A_2(x)} \frac{\partial}{\partial t} [u_{x2}(x,t)A_2(x)] \quad (10)$$

Equation of cochlear duct motion. To obtain this equation, it is assumed that the duct consists of independent elements of length Δx , each

possessing mass, elasticity, and friction. Alternately expressed, this amounts to the assumption that coupling along the cochlear duct takes place through the medium of the fluid in the scalae and not by mechanical attachment. The force across an element along the cochlea may be expressed as:

$$F_z(x,t) = F_1(x,t) - F_2(x,t) = m(x)\Delta x \frac{\partial u_z(x,t)}{\partial t} + f(x)\Delta x u_z(x,t) + k(x)\Delta x \int u_z(x,t)dt \quad (11)$$

This may be expressed in terms of pressure by dividing by the area, $b(x)\Delta x$, of the element along the cochlea.

$$P_z(x,t) = \frac{m(x)}{b(x)} \frac{\partial u_z(x,t)}{\partial t} + \frac{f(x)}{b(x)} u_z(x,t) + \frac{k(x)}{b(x)} \int u_z(x,t)dt \quad (12)$$

Combined equations of motion. The structure for the electrical analog of the cochlea is best obtained by first modifying the combined equations of motion into a different form. Since a lumped parameter electrical analog is to be used to simulate the distributed parameters of the cochlea, the equations of motion must first be expressed in terms of finite differences instead of differentials. Also, the equations should be in a form where the elements of the analog are obvious through direct term-by-term comparison. Equation 6 in terms of finite differences in the length, Δx , becomes:

$$u_z(x,t) = - \frac{3}{2} \frac{1}{b(x)} \frac{\Delta[u_{x1}(x,t)A_1(x)]}{\Delta x} \quad (13)$$

which, when put into the equation for motion of the cochlear duct, yields:

$$P_z(x,t) = - \frac{3}{2} \frac{m(x)}{b^2(x)} \frac{1}{\Delta x} \frac{\partial \Delta[u_{x1}(x,t)A_1(x)]}{\partial t} - \frac{3}{2} \frac{f(x)}{b^2(x)} \frac{1}{\Delta x} \Delta[u_{x1}(x,t)A_1(x)] \\ - \frac{3}{2} \frac{k(x)}{b^2(x)} \frac{1}{\Delta x} \int \Delta[u_{x1}(x,t)A_1(x)]dt \quad (14)$$

The equations for fluid motion, equations 9 and 10, may thus be rewritten as:

$$\Delta P_1(x,t) = \frac{f(x)\Delta x}{A_1(x)} [u_{x1}(x,t)A_1(x)] + \frac{\rho_p \Delta x}{A_1(x)} \frac{\partial}{\partial t} [u_{x1}(x,t)A_1(x)] \quad (15)$$

$$\Delta P_2(x,t) = \frac{f(x)\Delta x}{A_2(x)} [u_{x2}(x,t)A_2(x)] + \frac{\rho_p \Delta x}{A_2(x)} \frac{\partial}{\partial t} [u_{x2}(x,t)A_2(x)] \quad (16)$$

Equations 14, 15, and 16 will be used to compare the hydraulic-mechanical and electrical networks and to evaluate the electrical analog elements.

Electrical Analog of the Cochlea

There are several forms that the electrical analog of the cochlea may have, depending on the relations chosen for the analog equations. The

particular set chosen here provides certain practical conveniences in realization. The general cochlear analog section is shown in figure 5 which represents an element of length, Δx , along the cochlea. The equations are:

Equation of the shunt branch

$$e_z(x, t) = -L_p(x) \frac{\partial \Delta i(x, t)}{\partial t} - R_p(x) \Delta i(x, t) - \frac{1}{C_p(x)} \int \Delta i(x, t) dt \quad (17)$$

Equations of the series branches

$$\Delta e_1(x, t) = R_{s1}(x) i_1(x, t) + L_{s1}(x) \frac{\partial i_1(x, t)}{\partial t} \quad (18)$$

$$\Delta e_2(x, t) = R_{s2}(x) i_2(x, t) + L_{s2}(x) \frac{\partial i_2(x, t)}{\partial t} \quad (19)$$

Analog equations of correspondence. The following equations may now be directly compared:

equation 14 --- equation 17

equation 15 --- equation 18

equation 16 --- equation 19

and where the analog relations are:

pressure \longrightarrow voltage

volume velocity \longrightarrow current

The desired scaling relationships between the hydraulic-mechanical model of the cochlea and the proposed electrical model may be established by introducing the scale factor K_s and the impedance level factor K_z .

Voltage is defined as K_s times the pressure, and the electrical analog impedance is specified to equal K_z times the mechanical impedance level of the actual ear. Resulting equations are:

$$e_z(x, t) = K_s P_z(x, t) \quad (20)$$

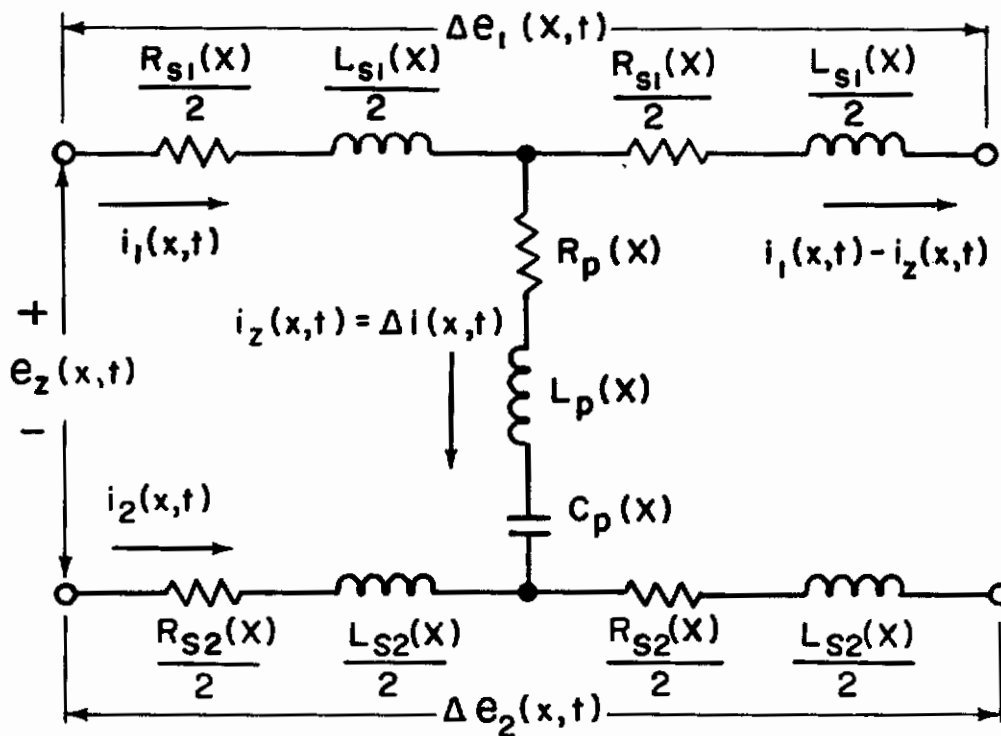
$$i_z = \Delta i(x, t) = \frac{K_s}{K_z} \frac{2}{3} b(x) \Delta x u_z(x, t) \quad (21)$$

$$\Delta e_1(x, t) = K_s \Delta P_1(x, t) \quad (22)$$

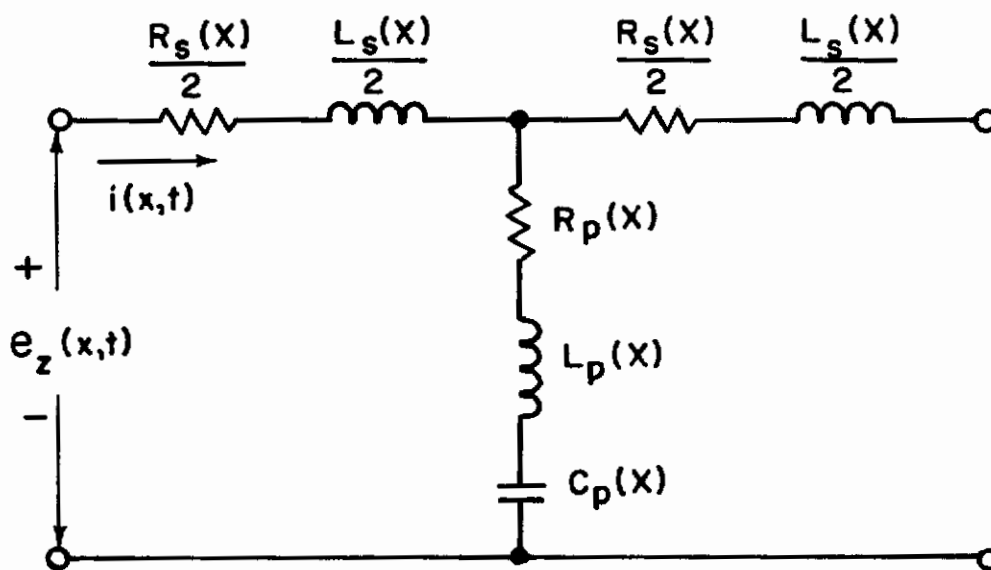
$$\Delta e_2(x, t) = K_s \Delta P_2(x, t) \quad (23)$$

$$\Delta i_1(x, t) = \frac{K_s}{K_z} \Delta [u_{x1}(x, t) A_1(x)] \quad (24)$$

$$\Delta i_2(x, t) = \frac{K_s}{K_z} \Delta [u_{x2}(x, t) A_2(x)] \quad (25)$$



a. One Section of the Cochlear Analog



b. Unbalanced Cochlear Analog Section

Figure 5. Basic Cochlear Analog Section

From the two sets of equations, the analogous elements of the electrical analog in terms of the cochlear model are:

$$R_{s1}(x) = K_z \frac{f_p(x)}{A_1(x)} \Delta x \quad (26)$$

$$R_{s2}(x) = K_z \frac{f_p(x)}{A_2(x)} \Delta x \quad (27)$$

$$L_{s1}(x) = K_z \frac{\rho_p}{A_1(x)} \Delta x \quad (28)$$

$$L_{s2}(x) = K_z \frac{\rho_p}{A_2(x)} \Delta x \quad (29)$$

$$R_p(x) = K_z \frac{3}{2} \frac{f(x)}{b^2(x)} \frac{1}{\Delta x} \quad (30)$$

$$L_p(x) = K_z \frac{3}{2} \frac{m(x)}{b^2(x)} \frac{1}{\Delta x} \quad (31)$$

$$C_p(x) = \frac{1}{K_z} \frac{2}{3} \frac{b^2(x)}{k(x)} \Delta x \quad (32)$$

For the unbalanced equivalent network of figure 5b, series (but not parallel) elements must be modified as:

$$R_s = R_{s1} + R_{s2} = K_z f_p \Delta x \left[\frac{1}{A_1(x)} + \frac{1}{A_2(x)} \right] \quad (33)$$

$$L_s = L_{s1} + L_{s2} = K_z \rho_p \Delta x \left[\frac{1}{A_1(x)} + \frac{1}{A_2(x)} \right] \quad (34)$$

which, under the assumption of equal areas for the scalae (ref. 2), become:

$$R_s = 2K_z \frac{f_p \Delta x}{A(x)} \quad (35)$$

$$L_s = 2K_z \frac{\rho_p \Delta x}{A(x)} \quad (36)$$

The velocity and displacement of the basilar membrane are found from the analog by measuring, respectively, the voltage across the resistor and the capacitor of the parallel branch. The voltage across the resistor is:

$$e_{R_p}(x, t) = i_z(x, t) R_p(x) \quad (37)$$

Contrails

Substituting for i_z from equation 21, and for R_p from equation 30, the velocity of any given point of the basilar membrane is given by

$$u_z(x,t) = e_{R_p}(x,t) \left[\frac{b(x)}{f(x)} \right] \frac{1}{K_s} \quad (38)$$

Similarly, the relation between capacitor voltage and displacement of the basilar membrane is

$$z(x,t) = e_{C_p}(x,t) \left[\frac{b(x)}{k(x)} \right] \frac{1}{K_s} \quad (39)$$

Sensory Loudness Conversion

With each analog section representing a length Δx of the cochlea, there is associated a loudness converter. The loudness converter function is analogous to that of a patch of hair cells, the associated nerve structures, and to some extent, sub-regions of the higher auditory centers. All of the loudness converters in combination form a simulation of the neural transduction process; their outputs form a subjective measure of the input to the analog ear.

Information is conveyed in the nervous system of the human by pulses. For a patch of neural cells, it is assumed that pulses occur in such profusion as to be adequately represented by continuous waveforms. Each cell, in response to an excitation, emits a series of monopolar pulses. The sum of the pulses from the various cells, as might be observed on a nerve, is the action potential. This potential shows a total pulse rate which is dependent upon the intensity of the excitation and, up to a maximum frequency, upon the frequency of the excitation. The average pulse rate response is such that it may be approximated by

$$H(s) = \frac{s\tau}{1 + s\tau} \quad (40)$$

where τ lies in the range of $1/2\pi(300)$ to $1/2\pi(3000)$ seconds (ref. 13).

The loudness converter may be represented by the block diagram of figure 6, where the blocks respectively represent the neural transmission effect as expressed by equation 40, a linear gain, a nonlinear rectification and power law process, and temporal averaging associated with the neural system.

Let $f(x,t)$ be a measure of the motion associated with a section of Δx of the cochlea at point x . The proposed loudness function (refs. 10,11,12) is

$$L(x) \approx K \text{Av} |f'(x,t)|^n = K \text{Av} |f(x,t) * h(t)|^n \quad (41)$$

where "Av" indicates a time averaging process, where $h(t)$ is the impulse response of $H(s)$, and where $*$ signifies convolution.

Subsequent analysis using the function of equation 41 shows that it models the sensory conversion system of the ear adequately, giving an explanation for masking and other psychoacoustic phenomena. It is possible to

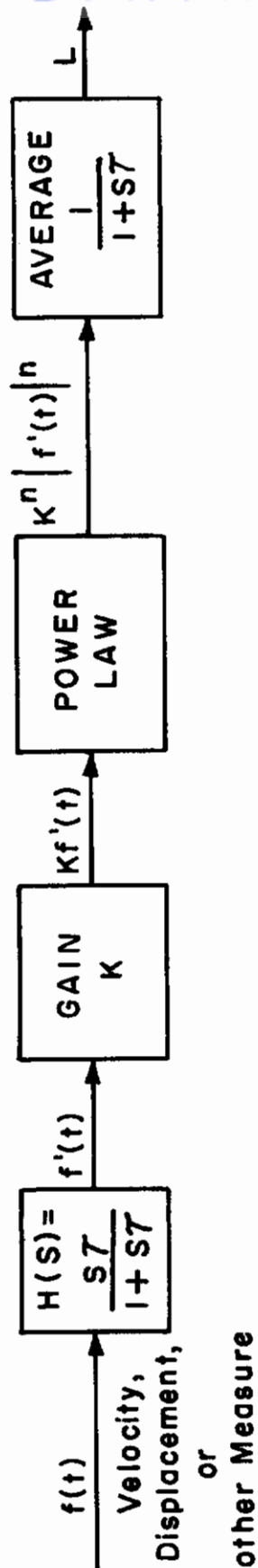


Figure 6. Loudness Converter Block Diagram

measure the power law exponent n by psychoacoustic tests which indicate that n is approximately equal to (or slightly larger than) unity, thus resulting in the loudness converters being approximately linear averaging (not envelope) detectors.*

Also of importance is the averaging time determined by the characteristics of the human hearing system. Although disputed among investigators, it is estimated to be about 0.2 second (ref. 14). This is adequately approximated by the first-order function $1/(1 + s\tau)$, where $\tau = 0.2$ second.**

Since the correct measure, $f(x,t)$, for loudness was initially unknown, provision was made in the analog to read the loudness conversion of velocity or displacement. Studies subsequently indicated that loudness depends on basilar membrane velocity with a value of $1/2\pi(1000)$ for τ of equation 40.

PARAMETERS OF THE COCHLEA

Introduction

To specify values for the electrical components of the analog cochlea, it is necessary to obtain numerical values for seven parameters. Three parameters are obtained directly from experimental data as presented by several investigators:

1. ρ_p : The density of the perilymph is given by Békésy as 1.034 (ref. 1).
2. $b(x)$: The width of the basilar membrane is given by Wever (ref. 13). A straight line approximation is $b(x) = .01 + \frac{.04}{3.5}x$, where b and x are in centimeters.
3. $A(x)$: The area of the scalae is given by Zwislocki (ref. 2). The two areas are assumed to be identical and are approximated by a straight line as $A(x) = .016 - \frac{.012}{3.5}x$, where A is in square centimeters and x is in centimeters.

The remaining four parameters are evaluated on the basis of theoretical calculations and experimental data. These parameters are:

4. $m(x)$: Dynamic mass per unit length of the cochlear duct.
5. $k(x)$: Dynamic stiffness per unit length of the cochlear duct.
6. $f(x)$: Dynamic friction per unit length of the cochlear duct.
7. $f_p(x)$: Equivalent friction per unit volume of the perilymph.

* Some investigators may employ mean-square values for sound stimuli. With mean-square measure, exponent values will be halved.

** Recent research in connection with modeling tonic-phasic neural behavior suggests the addition of a lead function to give $(1 + sa)/(1 + sb)$, where $a > b$ and $b \approx \tau$.

Dynamic Mass of the Cochlear Duct

Energy equivalent mass. The dynamic mass per unit length of the cochlear duct, $m(x)$, consists of the sum of two components, energy equivalent mass per unit length, $m_e(x)$, and loading mass per unit length, $m_l(x)$. The energy equivalent mass per unit length, $m_e(x)$, is defined as that mass per unit length which, when assigned to a point P at the center of the basilar membrane, possesses kinetic energy equal to that of the distributed mass of the entire cross-section of the cochlear duct under an assumed motion. The basic assumptions are:

1. Average density of the cochlear duct, ρ_D , is unity.
2. Materials composing the cochlear duct are incompressible.
3. Membrane distension is parabolic.
4. The cochlear duct cross-section can be approximated, as indicated in figure 7.

The method used to evaluate $m_e(x)$ is similar to that used by Zwislocki (ref. 2).

To evaluate the energy equivalent mass, the kinetic energy of the duct cross-section is written as

$$\text{Kinetic Energy} = T = T_a + T_b + T_c \quad (42)$$

$$T = \frac{1}{2} m_e(x) \left[\frac{d}{dt} (\text{displacement of point P}) \right]^2 \quad (43)$$

$$T = \frac{1}{2} m_e(x) v_P^2(x) \quad (44)$$

To obtain expressions for T_a , T_b , and T_c , the energies associated with section a, b, and c, a parabolic distension of the membrane is assumed, and the magnitude of this distension is determined for various regions in the cross-section of the duct.*

In cochlear duct section a, referring to figure 7, the displacement η_a is given by

$$\eta_a = 4A_R r(b_R - r) \quad (45)$$

where $A_R b_R^2$ is the maximum distension.

In the sections b and c, the displacement is

$$\eta = 4A_R \left[\frac{b_R}{B(z)} \right]^3 y(B(z) - y) \quad (46)$$

* In the following equations, the fact that the geometrical parameters of the duct cross-sections are functions of x , the distance along the cochlea, is not formally noted in order to simplify their writing.

where for the section associated with T_b

$$B(z) = b_c + z\left(\frac{b_R - b_c}{H}\right) \quad (47)$$

and for the section associated with T_c

$$B(z) = b + z\left(\frac{b_c - b}{h}\right) \quad (48)$$

The kinetic energies T_a , T_b , and T_c are

$$T_a = \frac{\rho_D}{2} \int_0^{b_R} \int_0^\theta r \left[\frac{d\eta_a}{dt} \right]^2 d\theta dr \quad (49)$$

$$= \frac{2}{15} \rho_D b^2 v_p^2 \theta \quad (50)$$

$$T_b = \frac{\rho_D}{2} \int_0^H \int_0^{B(z)} \left[\frac{d\eta_b}{dt} \right]^2 dy dz \quad (51)$$

$$= \frac{4}{15} \rho_D \left[\frac{H}{b_R - b_c} \right] b^2 v_p^2 \ln \left[\frac{b_R}{b_c} \right] \quad (52)$$

$$T_c = \frac{\rho_D}{2} \int_0^H \int_0^{B(z)} \left[\frac{d\eta_c}{dt} \right]^2 dy dz \quad (53)$$

$$= \frac{4}{15} \rho_D \left[\frac{h}{b_c - b} \right] b^2 v_p^2 \ln \left[\frac{b_c}{b} \right] \quad (54)$$

Therefore, the energy equivalent mass divided by $b^2(x)$ is

$$\frac{m_e(x)}{b^2(x)} = \frac{2}{v_p^2} [T_a + T_b + T_c] \frac{1}{b^2(x)} \quad (55)$$

$$= \frac{4}{15} \rho_D \left[\theta + 2\left(\frac{H}{b_R - b_c}\right) \ln\left[\frac{b_R}{b_c}\right] + 2\left(\frac{h}{b_c - b}\right) \ln\left[\frac{b_c}{b}\right] \right] \quad (56)$$

Loading mass. There is a mass loading of the cochlear duct due to transverse motion of the fluid surrounding the duct. To evaluate the magnitude of this effect, the equivalent loading mass is estimated from data obtained by von Békésy on a hydraulic model of the cochlea. This model had a cochlear partition of the same volume elasticity as that of a human cochlea and a width equal to that of the basilar membrane. This two-channel model was observed to have the same location of maximum displacement with frequency as for the human cochlea. Upon removing fluid from one channel, the maximum displacement could be maintained at a given position along the cochlea, before and after fluid removal from one channel, by increasing the excitation frequency by approximately 20 percent.

The cochlear partition may be assumed to consist of a series of independent elements, each possessing mass, elasticity, and friction. Thus, for a given point along the cochlear duct, the frequency of maximum displacement with fluid in only one scala, $\omega_m + \Delta\omega_m$, and the frequency of maximum displacement with fluid in both scalae, ω_m , can be related as:

$$\omega_m = \alpha \cdot \sqrt{\frac{k}{m_e + 2m_l}} \quad (57)$$

$$\omega_m + \Delta\omega_m = \alpha \cdot \sqrt{\frac{k}{m_e + m_l}} \quad (58)$$

where α relates to damping, which is approximately constant over the length of the cochlea. There results:

$$\left[\frac{\omega_m + \Delta\omega_m}{\omega_m} \right] = 1.2 \quad (59)$$

The loading mass due to one side of the cochlear duct is therefore determined as:

$$m_l(x) = 0.8 m_e(x) \quad (60)$$

In the actual ear, the basilar membrane and Reissner's membrane vibrate in phase below about 3000 cps, and thus the total loading mass is equal to the sum of the individual loading masses. This relationship has been assumed to hold over the total length of the duct.

Upon dividing by $b^2(x)$, equation 60 may be rewritten as:

$$\frac{m_l(x)}{b^2(x)} = 0.8 \frac{m_e(x)}{b^2(x)} \quad (61)$$

where $m_e(x)$ is given by equation 56. If it is assumed that the elemental mass loading increases as the square of the membrane width, the total loading mass becomes:

$$\frac{m_l(x)}{b^2(x)} = 0.8 \frac{m_e(x)}{b^2(x)} \left[1 + \left[\frac{b_R(x)}{b(x)} \right]^2 \right] \quad (62)$$

and the dynamic mass of the cochlear duct divided by $b^2(x)$ becomes:

$$\frac{m(x)}{b^2(x)} = \frac{m_e(x)}{b^2(x)} \left[1 + 0.8 \left[1 + \frac{b_R(x)}{b(x)} \right]^2 \right] \quad (63)$$

The calculated dynamic mass, $m(x)$, divided by $b^2(x)$, for a human cochlea is approximated by:

$$\frac{m(x)}{b^2(x)} = 4e^{-\frac{1.385}{3.5}x} \quad (64)$$

where x is in centimeters.

Dynamic Friction of the Cochlear Duct

The friction per unit length of the cochlear duct is due to both the friction of the duct itself and the viscous friction loading by the fluid in the scalae. The total friction is obtained from data taken by Békésy (ref. 1) on the logarithmic decrement.

If the cochlea is excited by short pulses, a damped oscillation is observed in the displacement of the basilar membrane. Békésy measured these oscillations in fresh specimens and found that the ratio of amplitudes between successive oscillation peaks of the same polarity was about 4:1 to 6:1 over the entire length of the basilar membrane. Using an average ratio of 5:1, the corresponding logarithmic decrement, D, is 1.6.

For a series RLC circuit as is associated with a section of the cochlea, the relationship between the logarithmic decrement and the circuit Q is

$$Q = \frac{\pi}{D \sqrt{1 - \left(\frac{D}{2\pi}\right)^2}} \quad (65)$$

Hence, since D is given as 1.6, the circuit Q is approximately 2. The dynamic friction of the cochlea, divided by $b^2(x)$, may thus be expressed as:

$$\frac{f(x)}{b^2(x)} = \frac{\pi \cdot m(x) \cdot f_0(x)}{b^2(x)} \quad (66)$$

where $f_0(x)$ represents the undamped resonant frequency.

In figure 8 are three curves showing the localization of frequency along the basilar membrane. These are: (1) localization of maximum displacement observed by Békésy, (2) localization of maximum velocity assumed for the development of the analog, and (3) localization of the maximum displacement and velocity as observed on the completed analog. The friction, divided by $b^2(x)$, as obtained using the assumed velocity localization curve therefore becomes

$$\frac{f(x)}{b^2(x)} = 2.6 \times 10^5 e^{-6.72 \frac{x}{3.5}} \quad (67)$$

where x is in centimeters.

Dynamic Stiffness of the Cochlear Duct

Previously calculated mass and the location of the maximum of velocity

Localization Curves

1. Observed on human cochlea ---Békésy (ref.1)
2. Assumed for development of electrical analog
3. Observed on the electrical analog

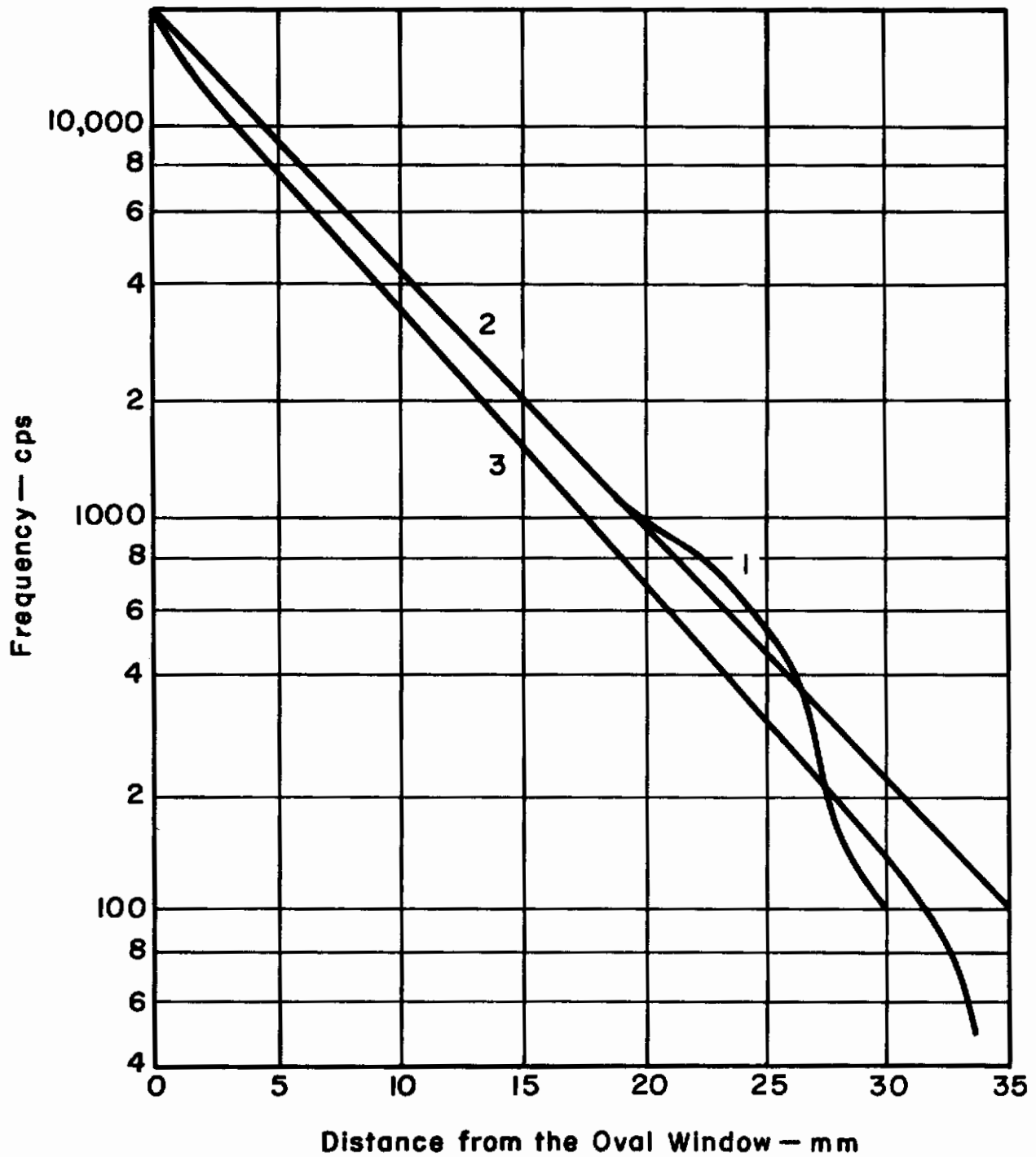


Figure 8. Pattern Localization

along the cochlear duct as a function of frequency may be employed in order to estimate dynamic stiffness. The expression for dynamic stiffness, divided by $b^2(x)$, is:

$$\frac{k(x)}{b^2(x)} = \omega_0^2(x) \frac{m(x)}{b^2(x)} \quad (68)$$

which becomes

$$\frac{k(x)}{b^2(x)} = 6.4 \times 10^{12} e^{-12 \frac{x}{3.5}} \quad (69)$$

where x is in centimeters.

This calculation for stiffness represents a significant departure from the approach of Zwislocki and others (ref. 2). Békésy employed a hair probe with a known buckling force to measure static elasticity in fresh specimens (ref. 1). These results are not believed to be correct for a dynamic model. It should be realized that the first-order electric model ignores mutual couplings between adjacent and remote sections. If the difference between static and dynamic values is anything like that found in certain kinds of distributed electric delay lines, use of Békésy's static values for the dynamic case is certainly wrong. The present analog can be expected to exhibit elasticity like that based on static data near the helicotrema (low frequency regions); near the stapes, however, elasticity characteristics can be expected to be quite different. The Appendix to this report considers relevant concepts of network approximation in more detail.

Equivalent Friction of the Perilymph

The method used to evaluate the equivalent friction of the perilymph is that of Zwislocki (ref. 2). It is assumed that each scala consists of a series of elementary tube sections of length Δx . Each of these cylindrical sections has constant cross-sectional area, equal to the area of the scala at that point.

For any one section of constant cross-sectional area, the velocity u_x as a function of the radius r is given by:

$$u_x(x, r) = \frac{p_0 - p_1}{4\mu\Delta x} (R^2 - r^2) \quad (70)$$

where p_0 and p_1 are the pressures on the two ends of an elementary tube section. Then the average velocity of flow through the tube is:

$$u_x(x) = \frac{1}{\pi R^2} \int_0^R 2\pi r u_x(x, r) dr \quad (71)$$

$$= \frac{p_0 - p_1}{8\mu\Delta x} R^2 \quad (72)$$

Contrails

The friction per unit volume for flow in an elementary tube section can be expressed as:

$$f_p(x) = \frac{\Delta \text{ force}}{\text{volume velocity} \cdot \Delta x} = \frac{(p_0 - p_1)A(x)}{\text{volume velocity} \cdot \Delta x} \quad (73)$$

$$f_p(x) = \frac{(p_0 - p_1)\pi R^2}{\left(\frac{p_0 - p_1}{8\mu\Delta x}\right)R^2(\pi R^2\Delta x)} = \frac{8\pi\mu}{\pi R^2} \quad (74)$$

$$= \frac{8\pi\mu}{A(x)} \quad \text{where } A(x) = \pi R^2 \quad (75)$$

where the coefficient of viscosity μ for the perilymph is 0.02. Thus $f_p(x)$ is closely approximated by:

$$f_p(x) = \frac{1}{2A(x)} \quad (76)$$

DESIGN OF THE COCHLEA

Number of Sections

The key to the design of an analog ear is the cochlea; it is this part of the ear that provides frequency analysis and, in addition, mechanizes conversion to neural signal form. The principal design problem is the choice for the number of RLC sections to be used in the circuit representation.

The pattern theory and knowledge of the Q of the cochlear duct (and hence the degree of pattern resolution) may be considered from the point of view of classical sampling theory. For $Q = 2$, half-octaves in frequency are appropriate for dividing the 100 - 20,000 cps range. About 13 half-octaves exist (and only six in the usual 300 - 3000 cps speech range), which implies that 13 is the minimum number of cochlear sections required for complete representation. The number actually selected was 36, which allows for a considerable "safety factor." Assumption of too few sections may introduce other sorts of errors than those related to patterns as, for example, reflections at junction points between sections.

In the last analysis, selection of the number of RLC sections is a matter of engineering judgment. Inasmuch as the end result demonstrates standard psychoacoustic phenomena and permits realization of bandwidth compression to less than 20 cycles per second, it is evident that the judgment originally employed was correct. Actually, good engineering judgment must be firmly based on suitable criteria for accuracy. According to the dictates of the pattern theory for hearing, notions from sampling theory may provide the only reasonable criterion. To assume need for a much larger number of sections than 36 suggests tacit acceptance of the old Helmholtz theory for hearing.

Impedance Scaling

The second design problem is impedance scaling from the basic analog

equations. The impedance scale factor K_z allows the electrical analog impedance level to be changed from that of^z the actual cochlea.

Selection of a practical value for K_z is facilitated if it is observed that the stiffness (equation 69) varies along the cochlea by about five orders of magnitude. By calculating the necessary range of capacitance and the related inductor size, it is possible to select a satisfactory compromise impedance scale factor.

A suitable value is $K_z = 1/40$, which yields maximum and minimum values of 6.66 μ f and 43 pf, respectively.*

Component Values

The electrical analog of the cochlea consists of a cascade of unbalanced RLC "tee" sections as illustrated in figure 5b. Thirty-six such sections with adjacent series elements combined give a single resistor and inductor between each element branch. The curves of figures 9, 10, and 11 present the information necessary for evaluating the elements of each section of the analog cochlea. Each curve is correct for $K_z = 1/40$. To determine the shunt elements, the curves of R , L , and C are read at points where x , the cochlear distance, is 0, 1, 2, ..., 35 millimeters.

It may be observed that the series coil Q requirements are impractical. An investigation (ref. 9) indicates that the series coil Q need be no greater than 20 over the frequency range of 100 to 10,000 cps in order to realize adequate accuracy.

THEORY AND DESIGN OF THE OUTER AND MIDDLE EAR

Introduction

Numerous studies of the mechanism of the middle ear have been published. Included are developments of electrical circuits for the simulation of specific functions such as input impedance (refs. 15,16) and circuits for the simulation of the complete mechanism (refs. 9,17,18,19). In figure 12 is shown a block diagram of the complete model of the outer and middle ear, as proposed in this paper. The analog circuit is developed on a direct basis by hypothesizing idealized mechanical and acoustic models for the various units and then realizing these models electrically. The analog shows a unique representation for the tympanic membrane and middle ear cavity and also shows means for including effects such as intratympanic reflexes and secondary transmission paths (ref. 9). Simplification of the general circuit results in a middle ear circuit which shows the input impedance and transfer function of a normal ear, and which is similar to that developed by Zwislocki (ref. 15) for the simulation of the input impedance.

* Throughout this paper, data on the human ear is given in cgs units; component values for the electrical analog are given in mks units. It is presumed that one cgs unit is numerically equal to one mks unit.

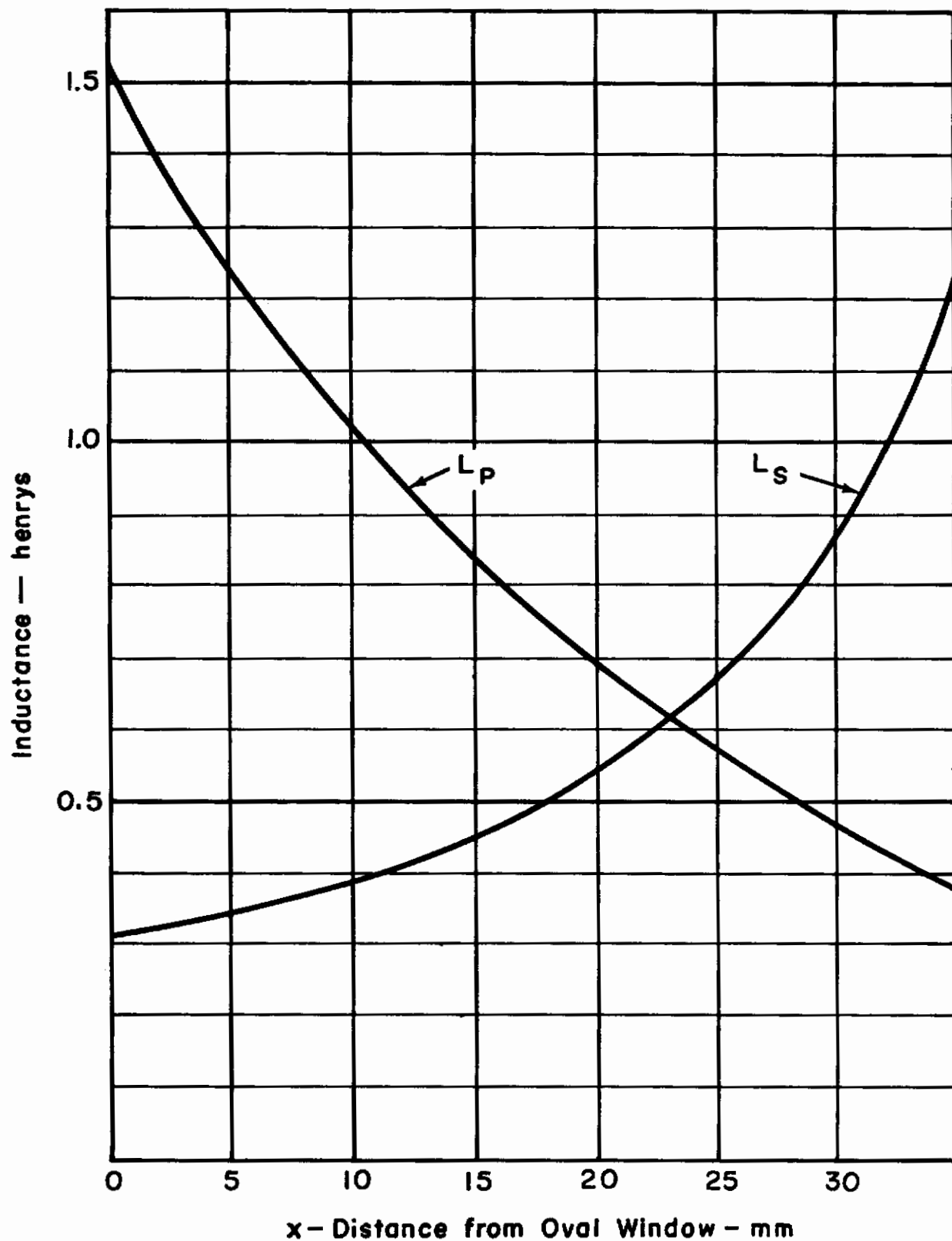


Figure 9. Parallel and Series Branch Inductance

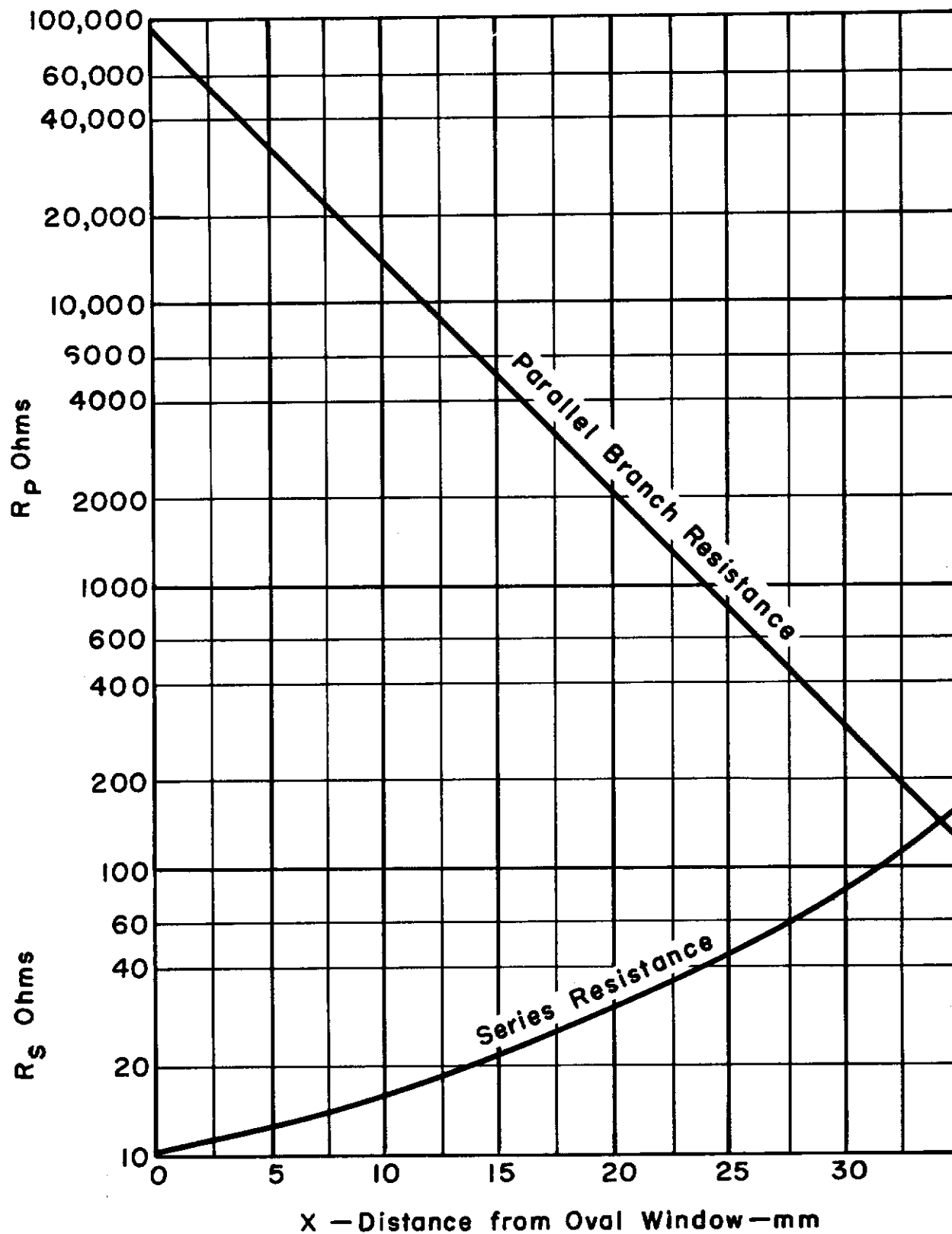


Figure 10. Series and Parallel Branch Resistance

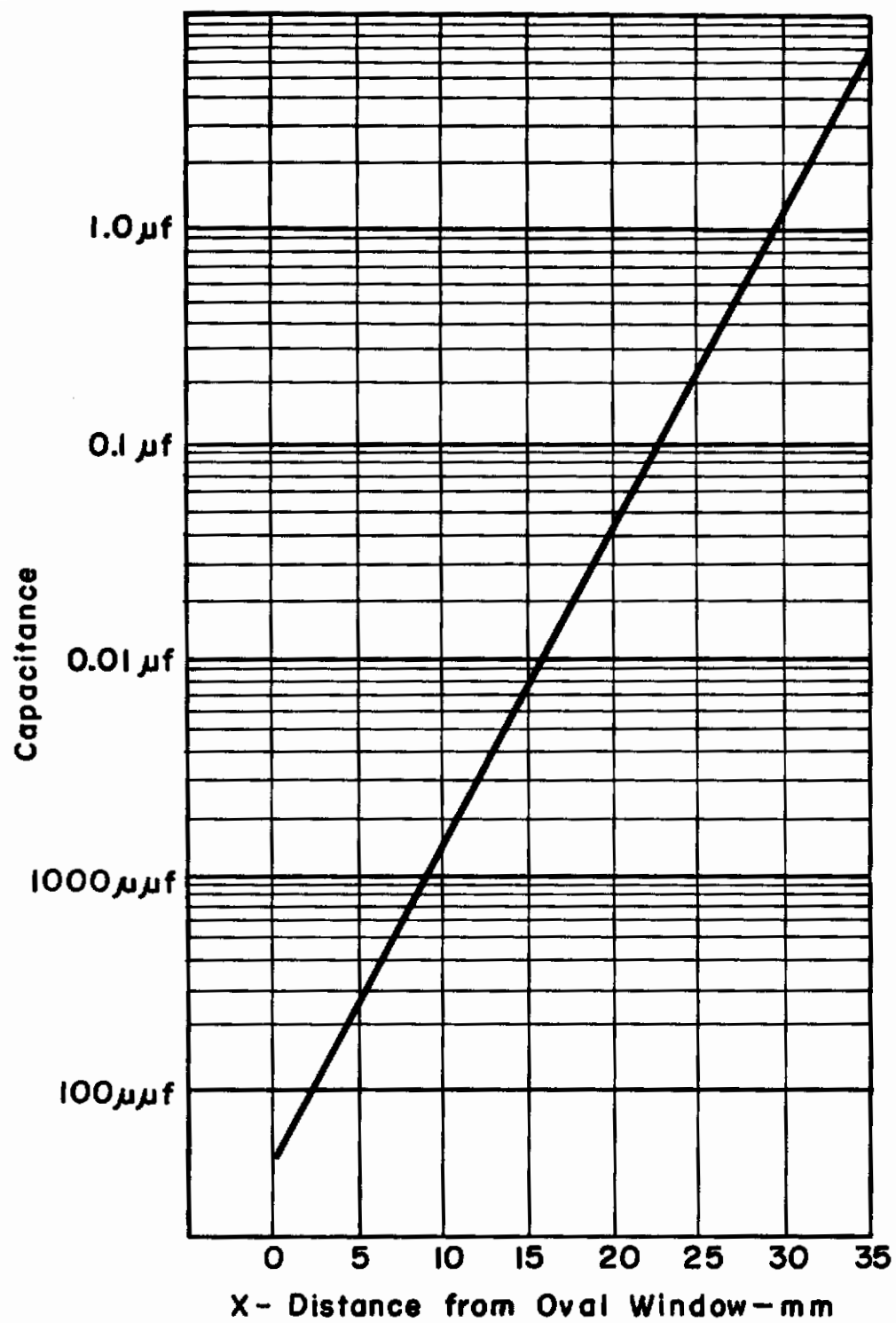


Figure II. C_p — Parallel Branch Capacitance

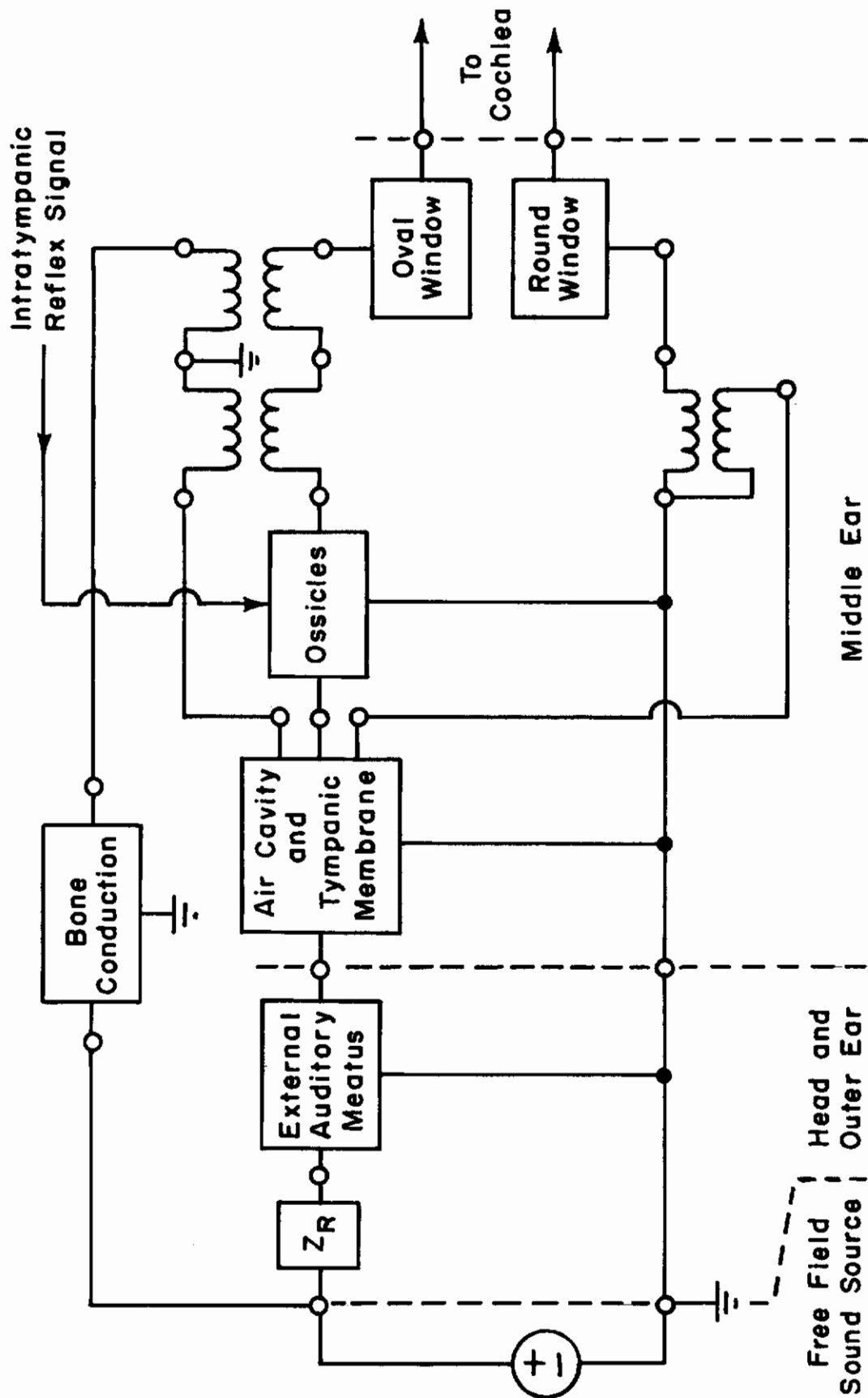


Figure 12. Block Diagram of the Outer and Middle Ear

Development of the Analog

The outer ear. The combined effect of the diffraction by the head and pinna, and the resonance of the external auditory meatus is to give an increased sound pressure at the tympanic membrane in reference to the free-field pressure. The average gain is a function of frequency and reaches a value of about 20 db at about 3000 cps. The increase in sound pressure due to the external meatus alone is about 10 db at about 4000 cps (ref. 20).

The effect of the head and pinna is simulated electrically by providing a radiation impedance in series between the signal generator, which represents the free-field sound source, and the input of the external meatus analog. The radiation impedance is not detailed here.

The external meatus is a tube having an average length of 2.7 cm and a cross-section area lying in the range of 0.3 to 0.5 sq cm (ref. 21). It is modeled by assuming a uniform tube of length $L = 2.7$ cm and cross-sectional area $A_m = 0.4$ sq cm. It is further assumed that plane waves exist in the meatus and that friction effects at the tube wall are negligible. The meatus can thus be electrically realized as a lossless, uniform transmission line. Using a pressure-voltage, volume velocity-current analog, the per unit length inductance and capacitance of the line are expressed in terms of acoustic parameters as:

$$L = K_z \frac{\rho_0}{A_m} \text{ henries} \quad (77)$$

$$C = \frac{A_m}{K_z \rho_0 c^2} \text{ farads} \quad (78)$$

where

c = velocity of sound in air.
= 34,400 cm per sec (20°C, 760 mm mercury)

ρ_0 = density of air.
= 0.00122 gm per cu cm (20°C, 760 mm mercury)

K_z = analog impedance level factor specified such that the electrical impedance level is equal to K_z times the acoustic impedance level.

The lumped parameter approximation to the analog of the external meatus may be realized as a cascade of either "tee" or "pi" low-pass sections. A sufficient number of sections must be used such that the lumped parameter line simulates the distributed parameter line over the frequency range of interest. An estimate of the required number of sections is obtained by considering the input impedance and transfer function poles under open circuit conditions. For a line 2.7 cm long, the transfer function poles occur at

$$f = 4100 \text{ n cps} \quad \left| \quad n = 1, 3, 5, 7, \dots \right. \quad (79)$$

and the input impedance poles occur at

$$f = 4100 n \text{ cps} \quad \left| \quad n = 0, 2, 4, 6, \dots \right. \quad (80)$$

Hence for a maximum frequency of 10,000 cps, it is estimated that at least three or four sections should be used.

The lumped parameter per section inductance and capacitance values are:

$$L \cdot \Delta x = \frac{K_z}{N} 8.23 \times 10^{-3} \text{ henries} \quad (81)$$

$$C \cdot \Delta x = \frac{1}{K_z N} 0.751 \times 10^{-6} \text{ farads} \quad (82)$$

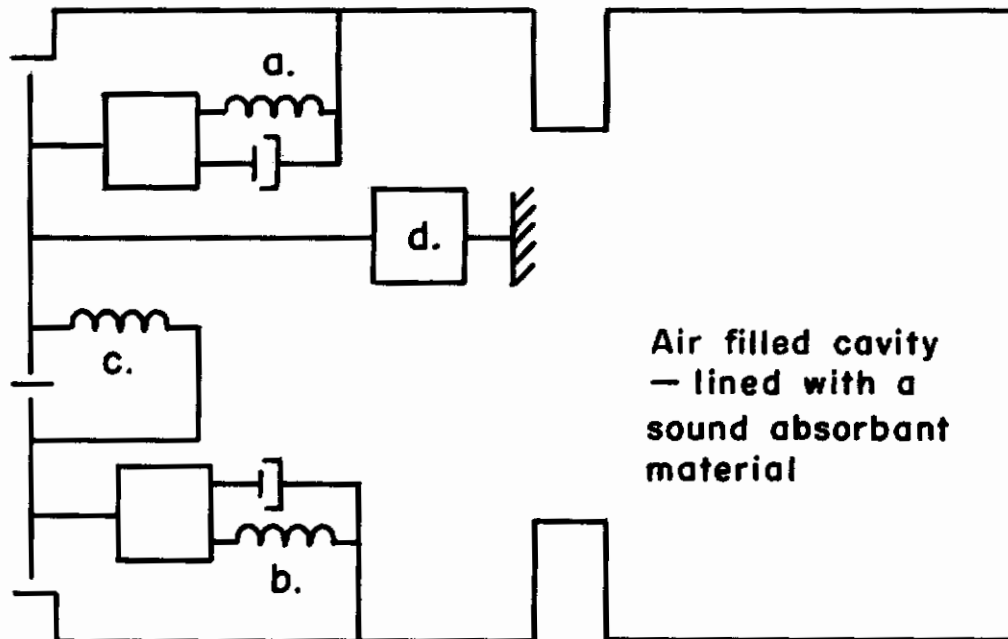
where N represents the number of sections. For a four-section line, these values are $2.05 K_z$ millihenries and $0.187/K_z$ microfarads.

The tympanic membrane and the middle ear cavity. The tympanic membrane is a light, flexible cone which closes the external meatus diagonally. It has a total area of about 0.85 sq cm, about 0.55 sq cm of which can be considered as being rigidly connected to the malleus (ref. 1).

The complete middle ear cavity consists of three interconnecting parts, the portion of the cavity which contains the ossicles, the antrum, and the mastoid cells. The total volume is about 2 cu cm, with that portion which contains the ossicles contributing about 0.5 to 0.8 cu cm. The mastoid cells vary greatly in size in different persons and are often so small that a portion of the complete cavity can be considered as being lined with a sound-absorbent material (ref. 1).

The tympanic membrane is modeled by assuming it to consist of individual sections which are elastically coupled and each of which possesses mass, friction, and elasticity. One of the sections is considered to be rigidly coupled to the malleus. This is illustrated in figure 13 for a two-section membrane representation. The parts of the middle ear cavity are considered to be lossy coupled resonators. The illustration of figure 13 shows a two-cavity representation where one resonator represents that part of the middle ear cavity containing the ossicles.

A pressure-voltage volume velocity-current analog is presented in figure 14 a. In this analog, L_m , R_m , and C_m represent respectively the mass, friction, and elasticity of the section of the tympanic membrane which is fastened to the malleus, and L , R , and C represent the mass, friction, and elasticity of the remaining part of the membrane. The membrane coupling is represented by the capacitor C_c and an ideal transformer. The size of the capacitor is dependent upon the degree of coupling between the two assumed sections of the membrane and the transformer ratio is dependent upon the relative sizes of the two sections. That the polarity of the transformer must be as shown may be noted from the fact that, if the air cavity is ignored and one section is given a displacement, the displacement of the other section must be in the same direction.



- a. The part of the tympanic membrane connected to the ossicles
- b. The part of the tympanic membrane not connected to the ossicles
- c. Tympanic membrane coupling
- d. The ossicles and the cochlea

Figure 13. Model of the Tympanic Membrane and the Middle Ear Cavity

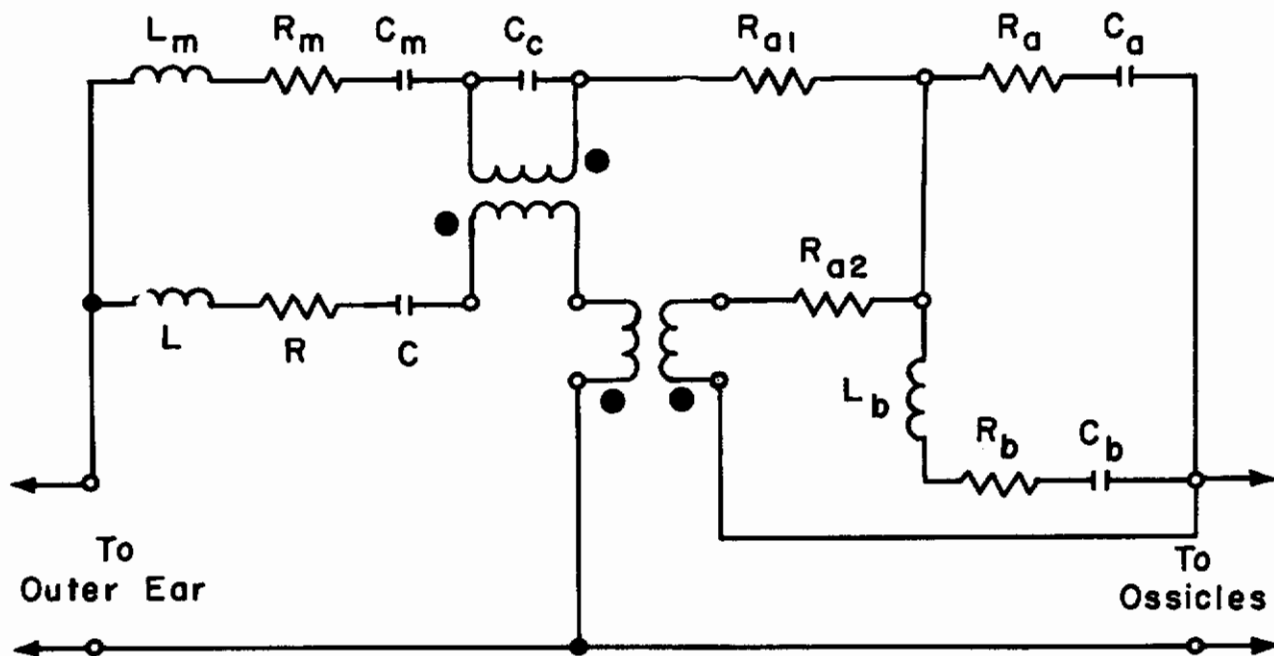


Figure 14a.

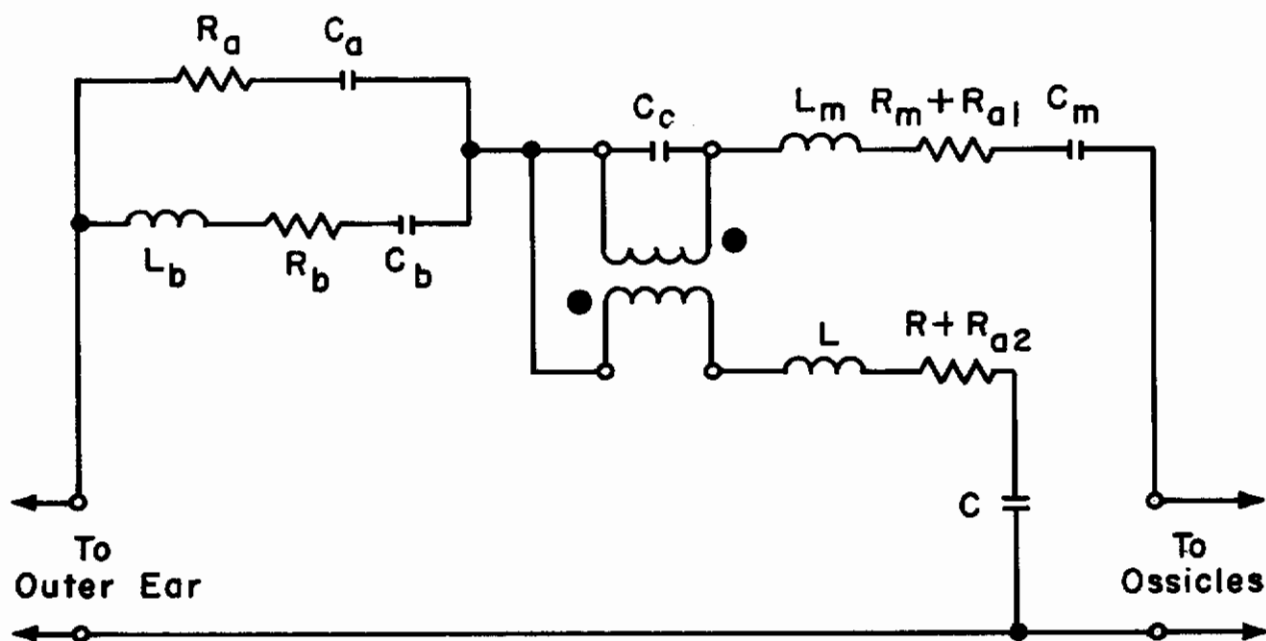


Figure 14 b.

Figure 14. Electrical Analog of the Tympanic Membrane and the Middle Ear Cavity

Contrails

The loading of the air cavity upon the membrane sections and the coupling between the sections due to the cavity are represented by resistances R_a , R_{a1} , R_{a2} , and R_b , the inductance L_b , the capacitances C_a and C_b , and the ideal transformer associated with these components. The transformer must have a polarity as indicated and the ratio must be one-one. This may be noted from the fact that, if the air is considered incompressible, and if one of the sections is displaced, there must result an equal but negative volume displacement of the other section. The cavity representation is based upon the assumption that, if the sections move in phase, there will result a fluid motion throughout the cavity, whereas if the sections move in phase opposition, there will be negligible fluid motion at all points in the cavity except near the membrane sections; elastance effects under the latter condition are ignored and only losses are shown.

It is noted that the location of the various parts of the tympanic membrane and middle ear cavity representation of figure 14a can be interchanged. Hence, an ideal transformer can be removed, resulting in the simplified structure of figure 14b.

The ossicles and the cochlear windows. The ossicles act as a set of mechanical levers which provide a force amplification of about 1:1.3 between the tympanic membrane and the oval window. The malleus fastens to the tympanic membrane. The malleus and the incus are united by a stiff joint and are supported by several ligaments. The stapes is connected to the long process of the incus by means of a flexible joint. The footplate of the stapes nearly closes the oval window and is connected to the bone surrounding the window by means of a flexible annular ligament. Under normal conditions, motion of the tympanic membrane causes a rotation of the ossicles about an axis which is located at approximately their center of gravity. This causes a motion of the stapes; hence sound energy is transmitted to the cochlea.

Two muscles are associated with the middle ear, the tensor tympani muscle which attaches to the malleus, and the stapedius muscle which attaches to the posterior part of the neck of the stapes. These two intratympanic muscles contract in response to high sound intensities so as to modify the characteristics of the middle ear structure and as a result to reduce the transmission properties of that structure. At low sound intensities these muscles are presumed to contribute only constant mass, elastance, and friction effects to the middle ear structure.

A hypothesized mechanical model for the ossicles and the cochlear windows is shown in figure 15. In order to obtain this model, it is assumed that the middle ear behaves linearly and hence also that low sound intensity conditions apply.

The electrical analog of this system is shown in figure 16. The following analog representations are employed, with necessary transformations between these obtained by means of ideal transformers.

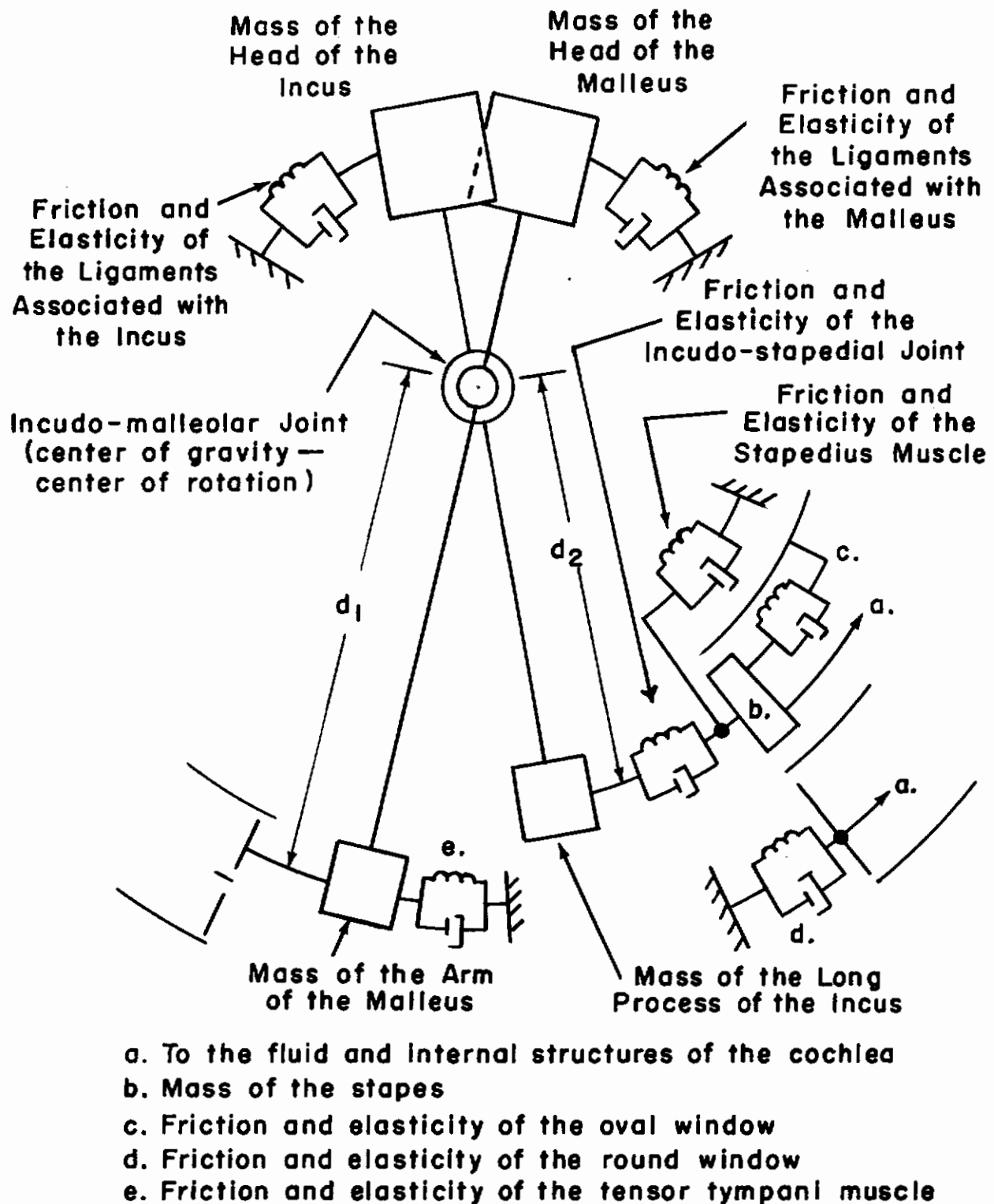


Figure 15. Model of the Ossicles and the Cochlear Windows

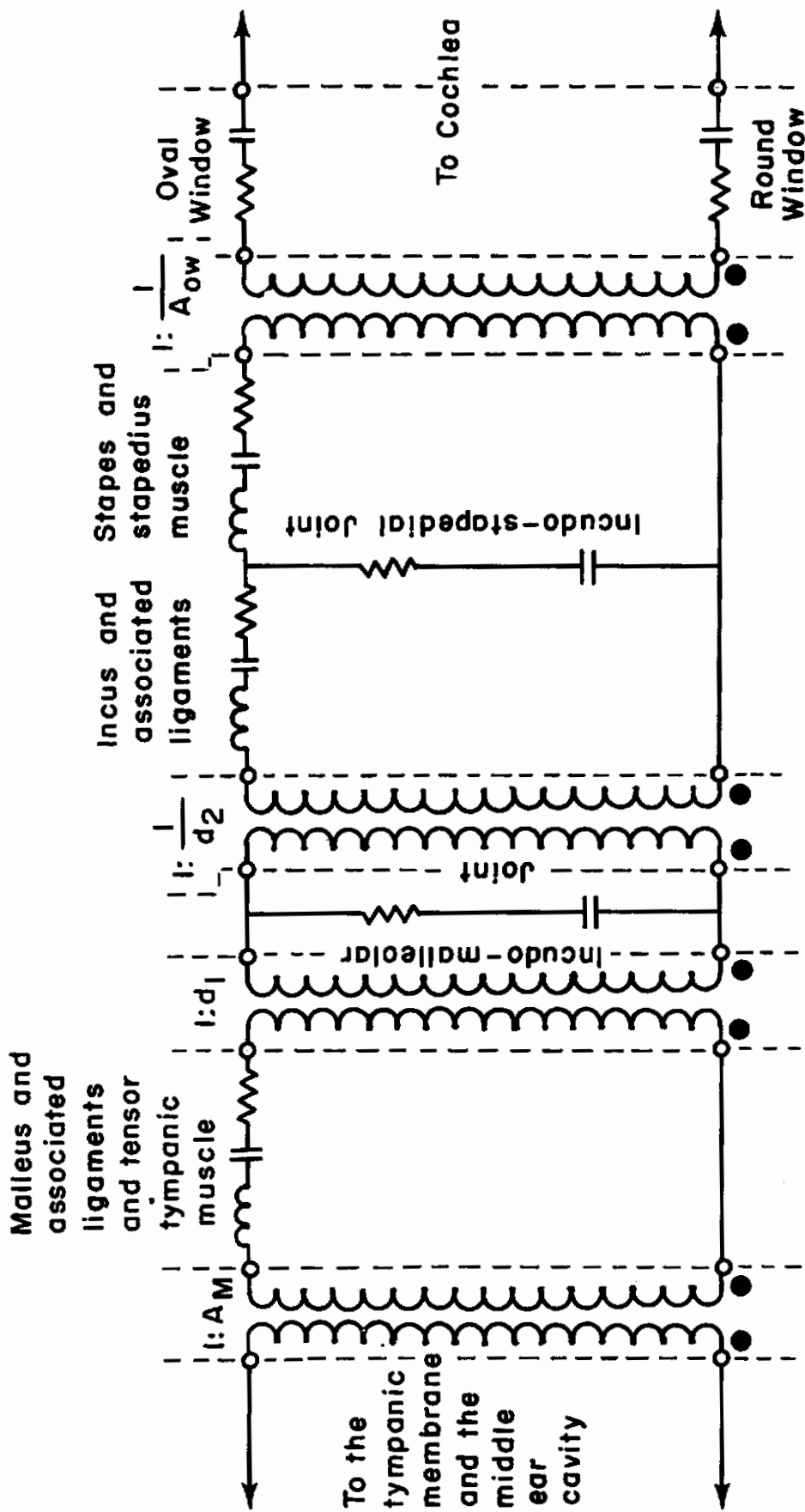


Figure 16. Electrical Analog of the Ossicles and the Cochlear Windows

Electrical System

1. voltage
current

2. voltage
current

3. voltage
current

Mechanical System

force
linear velocity

pressure
volume velocity

torque
angular velocity

Other conduction paths and intratympanic reflexes. The effects of conduction paths other than those of the ossicles and the effects of the intratympanic reflexes are relatively unimportant in hearing at normal speech intensities. The inclusion of these effects is considered only with reference to the general block diagram shown in figure 12.

There exist two means of transmitting sound energy to the cochlea other than the path provided by the ossicles. One means is conduction resulting from the air in the middle ear cavity and the other is bone conduction. In the process of air conduction, a sound pressure in the middle ear cavity drives both the oval and round windows. The effectiveness depends upon the pressure difference between the windows which, in turn, depends upon the form of the cavity. This method of transmission can be simulated as shown in figure 12. The actual circuit representation for the middle ear cavity is, however, necessarily more complex than that shown in figure 14 so as to provide phase and magnitude differences in pressure at the windows.

Sound transmission to the cochlea by means of bone conduction results from vibrations of the skull. Békésy (ref. 1) has shown that bone conduction tones can be completely canceled by tones received through the middle ear. Hence, bone conduction can be considered in terms of an equivalent excitation at the cochlear windows and its effects can thus be included in the analog by means of the method shown in figure 12. It is noted, however, that the block which represents the bone conduction transfer function is quite variable since it is dependent upon such factors as whether the skull is vibrated by air-borne sounds or by contact with a vibrating body, and if the latter, at what point on the skull the contact is made. If the transfer function is known for conduction by the ossicles, which is presumed to be the case at least for the analog, then Békésy's method of bone conduction tone cancellation can be used to determine the bone conduction transfer function.

The tensor tympani muscle and the stapedius muscle move ossicles and stiffen membranes as a result of hearing a relatively intense sound so as to decrease the transmission properties of the middle ear. This constitutes a feedback device. However, unlike the simple servomechanism or automatic gain control, feedback affects the values of the system parameters.

The lumped parameter middle ear network shows components which related one-to-one with ossicles and membranes. It thus appears possible to isolate parameters for control. The controlling signal is dependent upon the loudness of the sound and is fed back from a part of the complete analog ear which provides a measure of this loudness.

Practical Realization of the Analog

Simplification of the analog. Sufficient physiological data is not available to specify all component values for the middle ear analog. Therefore, a simplified form of the analog can be developed with component values specified only so as to provide input impedance and transfer functions similar to those of the normal human ear.

A simplified middle ear analog similar in structure to that proposed by Zwislocki (ref. 15) requires that three assumptions be made. First, it is presumed that the effects of air cavity and membrane coupling cancel and hence that the air cavity can be represented by a single capacitor of appropriate size; the cavity and membrane representations can thus be replaced by short circuits. Second, the incudo-malleolar joint is presumed to be rigid and hence the analog representation becomes an open circuit. Third, the mass and friction effects associated with the stapes, the stapedius muscle, and the windows are presumed to be negligible with respect to the input impedance of the cochlea.

The complete simplified analog is shown in figure 17 where all ideal transformers associated with the ossicles are combined into a single unit. Values in parenthesis indicate an impedance level change by a factor of 40 so as to concur with the impedance level change of the analog cochlea.

Physiological data used for the determination of component values come from the investigations of Békésy (ref. 1) and Zwislocki (ref. 15), with the final criterion for the determination being the simulation of the input impedance and transfer function of the normal human ear.

The transformer ratio is obtained by using the area of the oval window, $A_{ow} = 0.032$ sq cm, the area of the part of the tympanic membrane which is considered to be rigidly coupled to the malleus, $A_m = 0.55$ sq cm, and the lever arm ratio of the ossicles, $d_1/d_2 = 1/1.3$. The resulting ratio is $1/22.4$.

An estimate of the capacitance which represents the windows and the stapedius muscle is obtained from Békésy's data on the volume displacement of the windows. This data indicates a capacitance for the windows of $0.0005 \mu\text{fd}$; this figure is an upper limit since it does not include the effects of the stapedius muscle. Experimental adjustment such that the analog simulated the transfer function of a normal human ear specified the capacitance shown in figure 17.

Values of the eight components which represent the tympanic membrane and the ossicles are obtained using input impedance data for both normal and otosclerotic ears and transfer function data for an ear with the stapes immobilized. These data and the results obtained from the analog are presented in the next section.

Input impedances and transfer functions. The input impedance magnitude for the four-section external auditory meatus analog is shown in figure 18 for the case where the analog is terminated by the middle ear analog.

In figure 19 are shown the real and the reactive parts of the input impedance to both normal and otosclerotic middle ears as observed by Zwislocki,

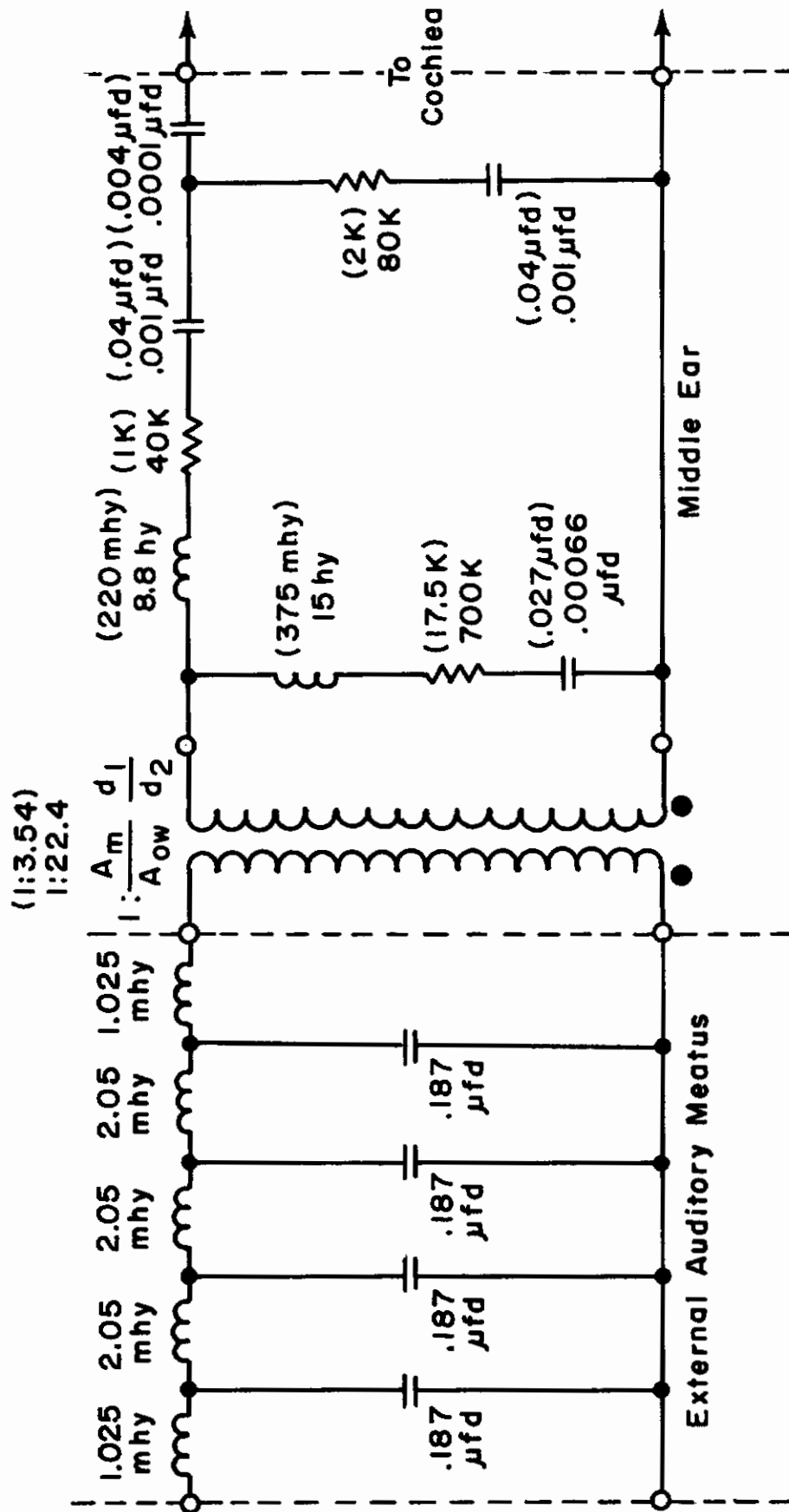


Figure 17. Simplified Analog of the Outer and Middle Ear

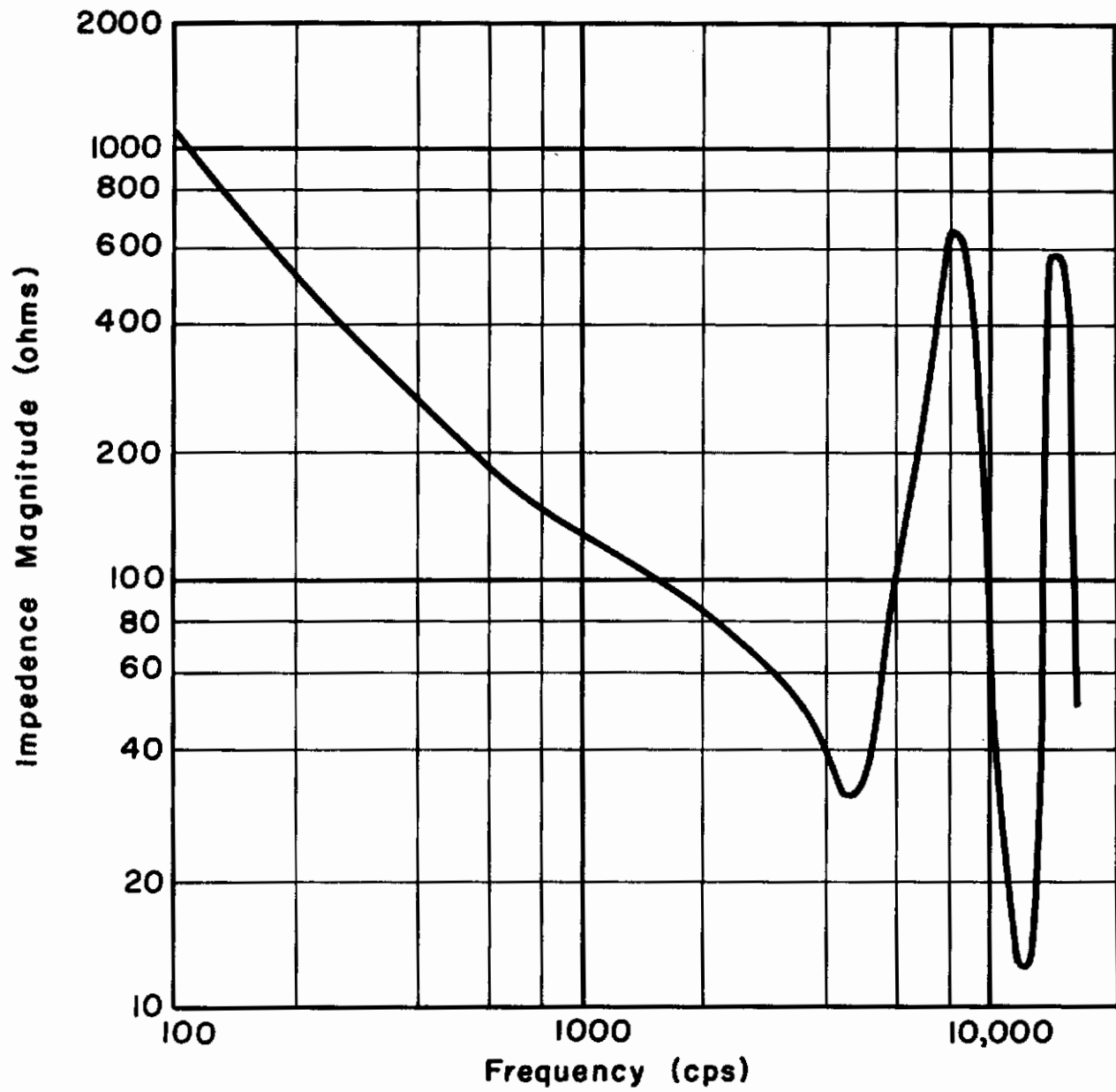


Figure 18. Input Magnitude of the External Auditory Meatus

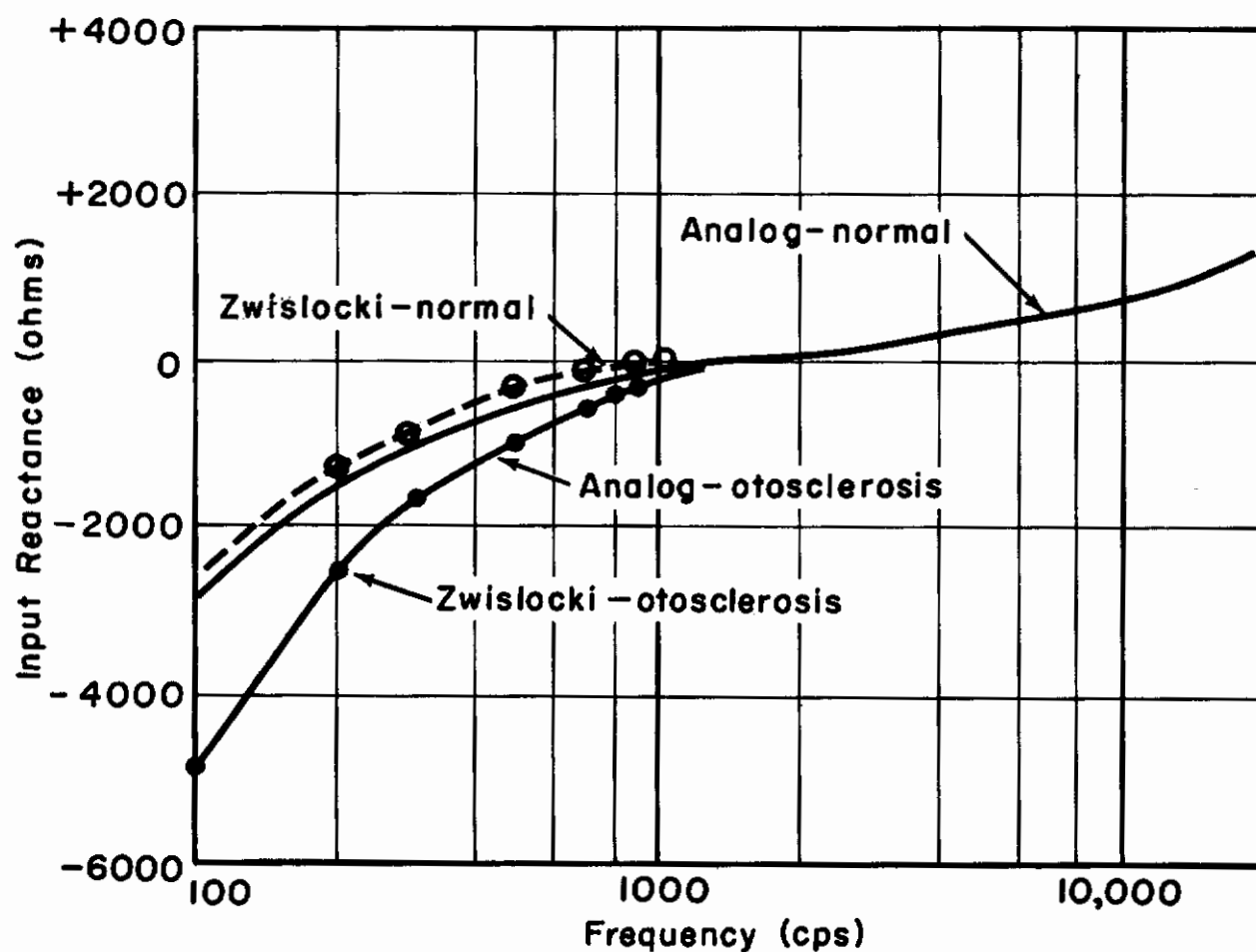
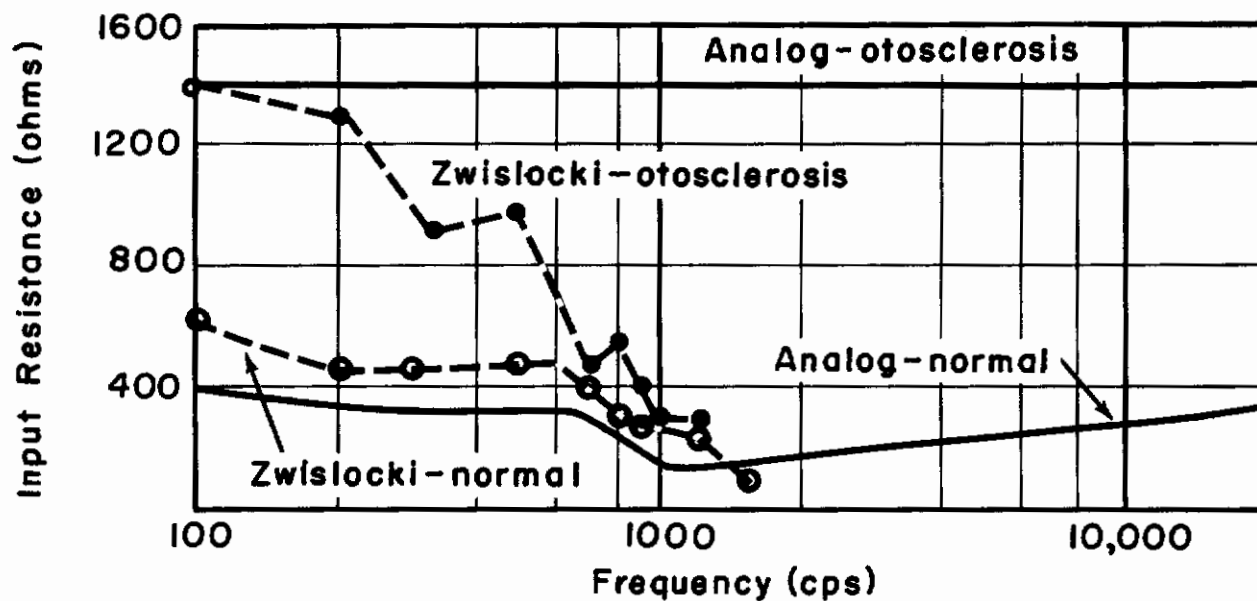


Figure 19. Input Impedance of the Middle Ear

and the real and reactive parts of the input impedance to the middle ear analog. It is noted that, although the analog simulates the input impedance to the normal ear, it does not simulate the input resistance to the otosclerotic ear except at low frequencies. An otosclerotic ear is one in which the stapes and the incudo-stapedial joint become more or less immobilized as a result of a bony growth (ref. 22). The corresponding analog representation is an open circuit for both the incudo-stapedial joint and the stapes. Under this pathological condition, the simplified analog is inadequate; suitable representation requires use of the more detailed circuits analogs of figures 14 and 16.

The transfer function magnitude of the four-section external meatus analog is shown in figure 20. Also shown is the magnitude of the transfer function from the entrance of the meatus to the meatus side of the tympanic membrane as observed in human ears by Wiener and Ross (ref. 20).

Various transfer functions for both the human ear and the analog ear are shown in figure 21. Curve number 1 gives the pressure transfer function of a human ear from the meatus side of the tympanic membrane to the cochlea side of the stapes under the condition of an immobilized stapes. This curve is given by Békésy (ref. 1). Curve number 2 gives the same transfer function as observed in the middle ear analog; the analog representation for the immobilized stapes is an open circuit. Curve number 3 gives the pressure transfer function of a normal ear from the meatus side of the tympanic membrane to the cochlea side of the stapes. This data is given by Fletcher (ref. 23) as deduced from experimental data given by Békésy. Curve number 4 gives the same transfer function for the analog. Curve number 5 shows the analog pressure transfer function from the entrance of the meatus to the cochlea side of the stapes.

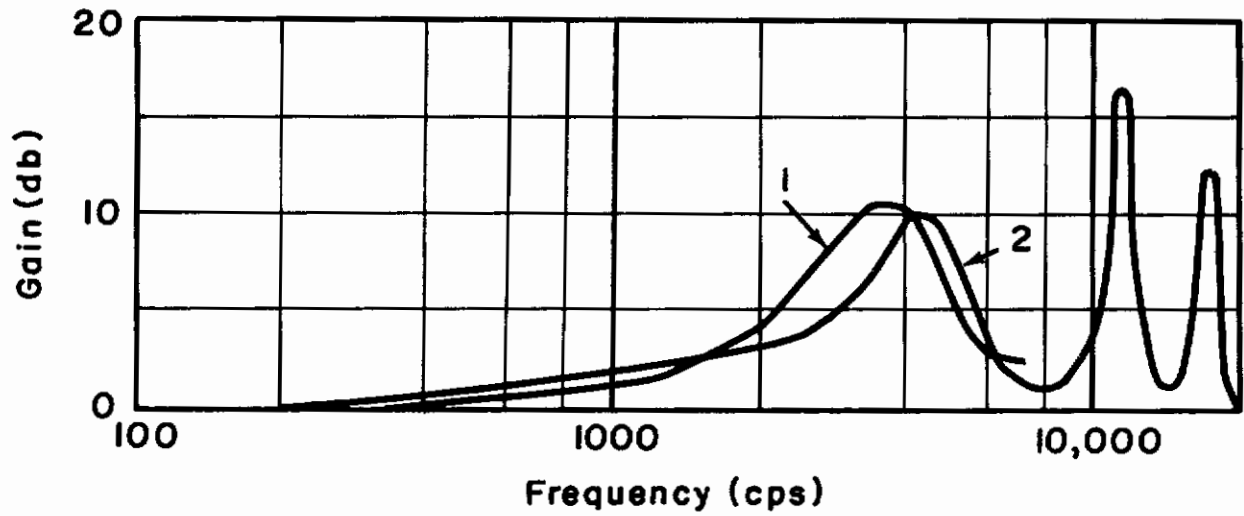
DESIGN AND RESULTS

The Complete Analog Ear

The hearing system as modeled in the previous chapters includes the outer and middle ear, the cochlea, and part of the neural structure of the cochlea and the higher auditory centers. A practical analog system requires in addition, input and readout equipment. The analog system as realized in this investigation is illustrated in figure 22. Signals representing displacement, velocity, or loudness associated with points along the basilar membrane are represented by a spatial array of outputs along the cochlea. A commutator converts the spatial array to a temporal pattern for display on an oscilloscope or for application to recognition devices. It is desirable that the sampling rate be sufficiently high so that the patterns portray the distinguishable characteristics necessary for speech recognition. To accomplish this, a mercury jet commutator is used which samples all 36 sections of the cochlea in 18 milliseconds, and provides complete patterns at the rate of either 20 or 40 per second.

Input Impedance

The analog cochlea exhibits approximately the same input impedance as the human cochlea; the magnitude and phase characteristics for the analog are



- 1. Wiener and Ross
- 2. 4 Section Analog

Figure 20. Transfer Function Magnitude of the External Auditory Meatus

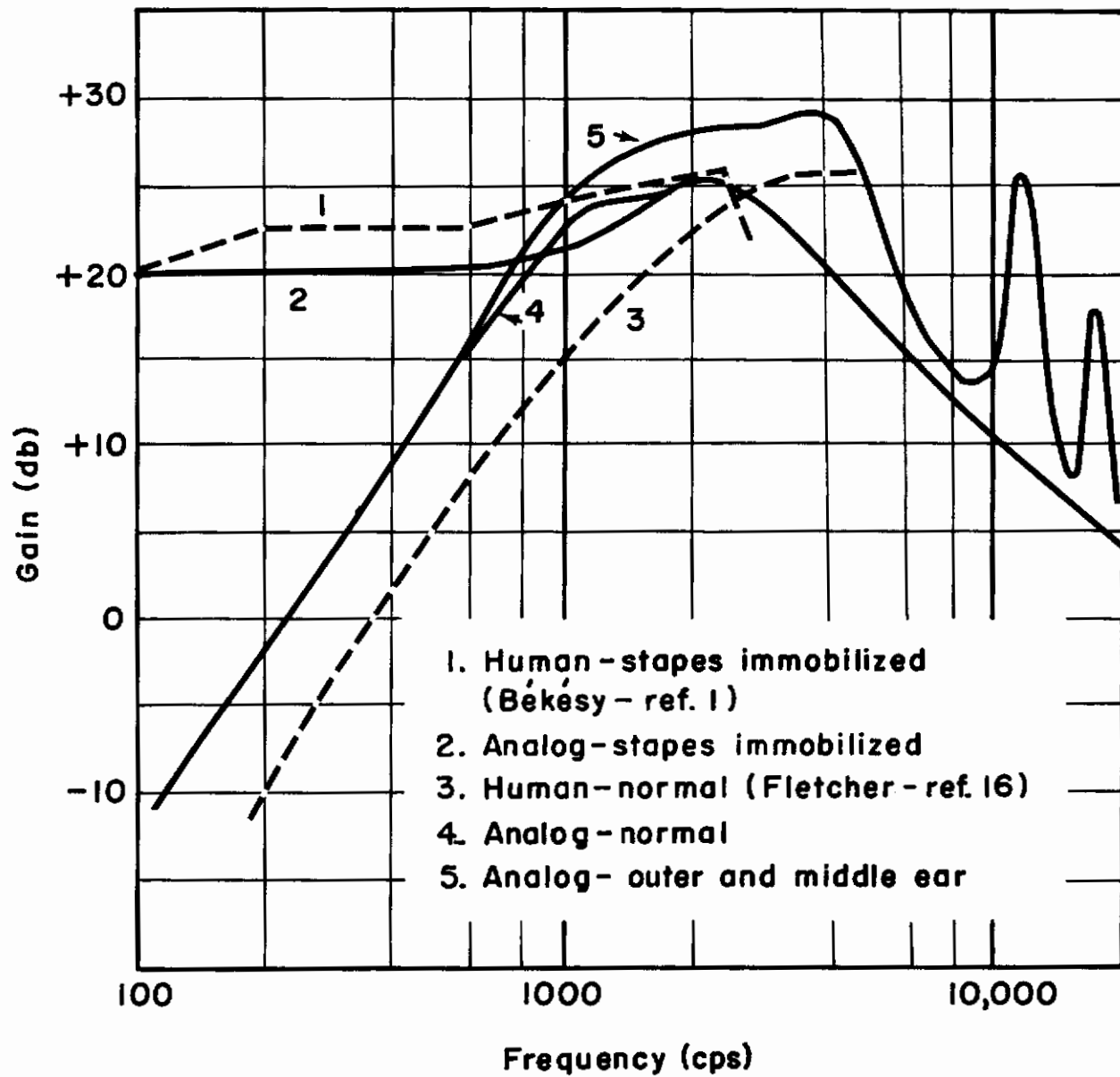


Figure 21. Transfer Functions of the Middle Ear

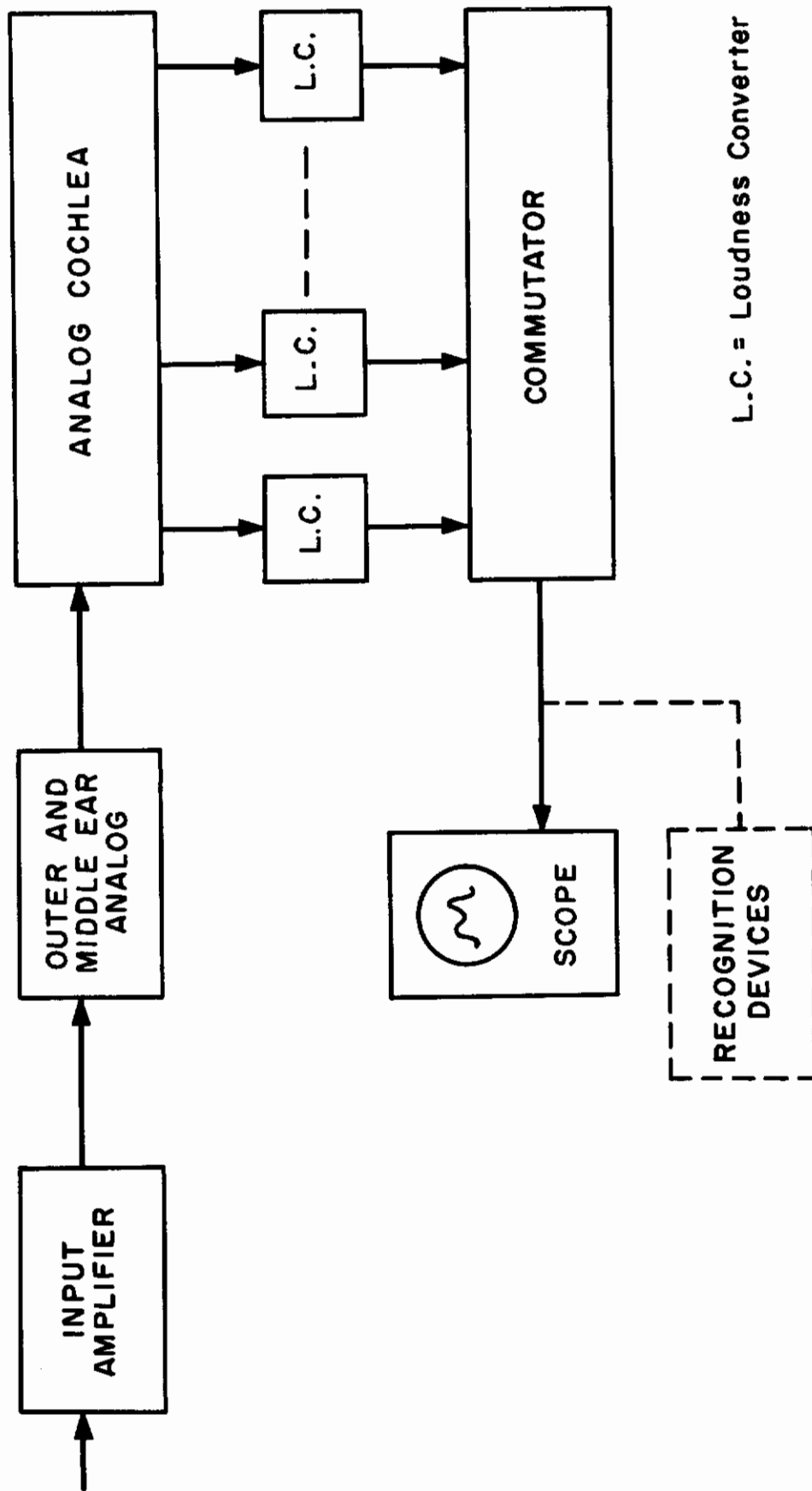


Figure 22. Block Diagram of the Ear

presented in figure 23. One scale presents the impedance of the analog in ohms. The other scale presents the impedance of the analog converted to the impedance level of the direct model of the human cochlea. In figure 23 is also shown the input impedance magnitude for the human cochlea as obtained from experimental data given by Békésy (ref. 1).

In order to facilitate use of the external and middle ear analog, it is desirable to provide a circuit which simulates the input impedance of the cochlea. A suitable circuit is shown in figure 24.

Velocity and Displacement of the Basilar Membrane

The velocity and displacement of the basilar membrane for a sinusoidal excitation of the analog cochlea are each a function of frequency and the distance along the cochlea. The data is presented in figure 25 in terms of the normalized magnitude characteristics and the displacement phase characteristics. For a sinusoidal excitation, the normalized velocity and the normalized displacement patterns are identical; the velocity pattern magnitude differs from the displacement pattern magnitude by a factor of ω which normalization removes.

In figure 25 are also shown, for comparison purposes, low frequency normalized displacement magnitude and displacement phase characteristics as observed by Békésy (ref. 1) on a human cochlea.

Curve number 3 in figure 8 shows the location along the analog cochlea of the peak magnitudes of the velocity patterns and the displacement patterns as a function of signal frequency. A difference in the location of the peak magnitude of a velocity pattern and a displacement pattern of the same frequency could not be noted.

Loudness Phenomena

In the analog ear, a single loudness converter can provide only place and loudness converted sound intensity information. The output of an individual loudness converter, $L(x)$, is thus considered to represent the loudness associated with the corresponding segment of the cochlear duct. The total loudness, $L_T(x)$, is considered to be the sum effect of the individual loudness as:

$$L_T(x) = \sum_x L(x) \quad (83)$$

The characteristic of the basilar membrane motion which is of importance in hearing is not known. To provide an indication as to whether velocity or displacement is the important characteristic and also to estimate the value of τ for equation 40, loudness was measured as a function of frequency using both the velocity and the displacement of the basilar membrane and also using frequencies of 300 cps, 1000 cps, and 3000 cps for $1/2\pi\tau$. This data is presented in figure 26.

On the basis of a comparison of the various curves in figure 26 with threshold of hearing curves, the velocity of the basilar membrane is selected

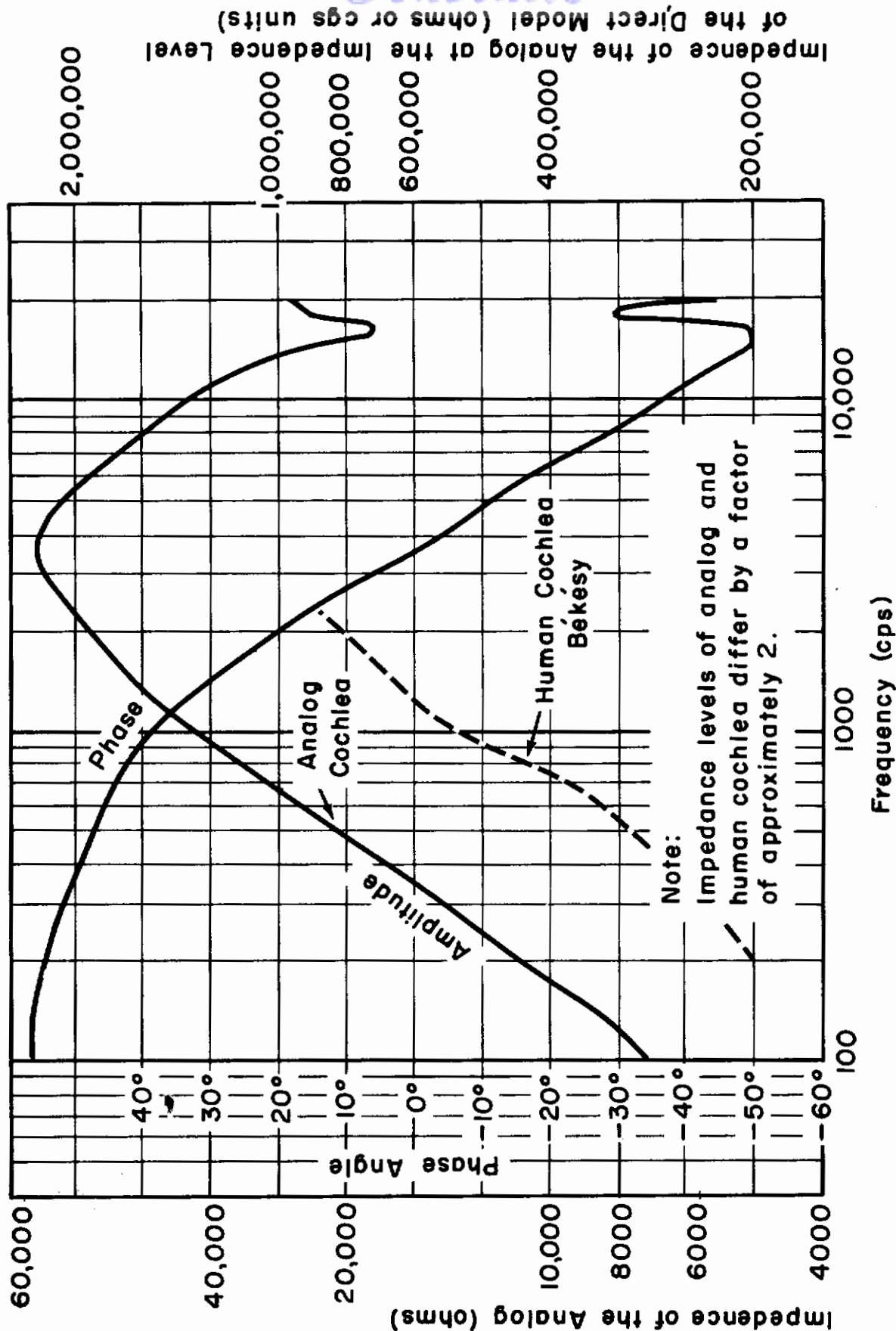


Figure 23. Input Impedance Phase and Magnitude of the Analog Cochlea

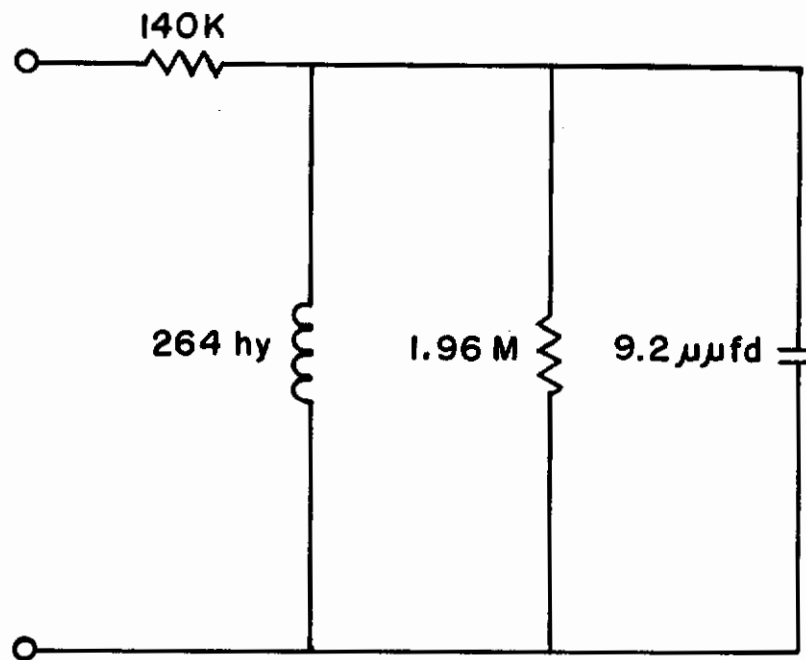
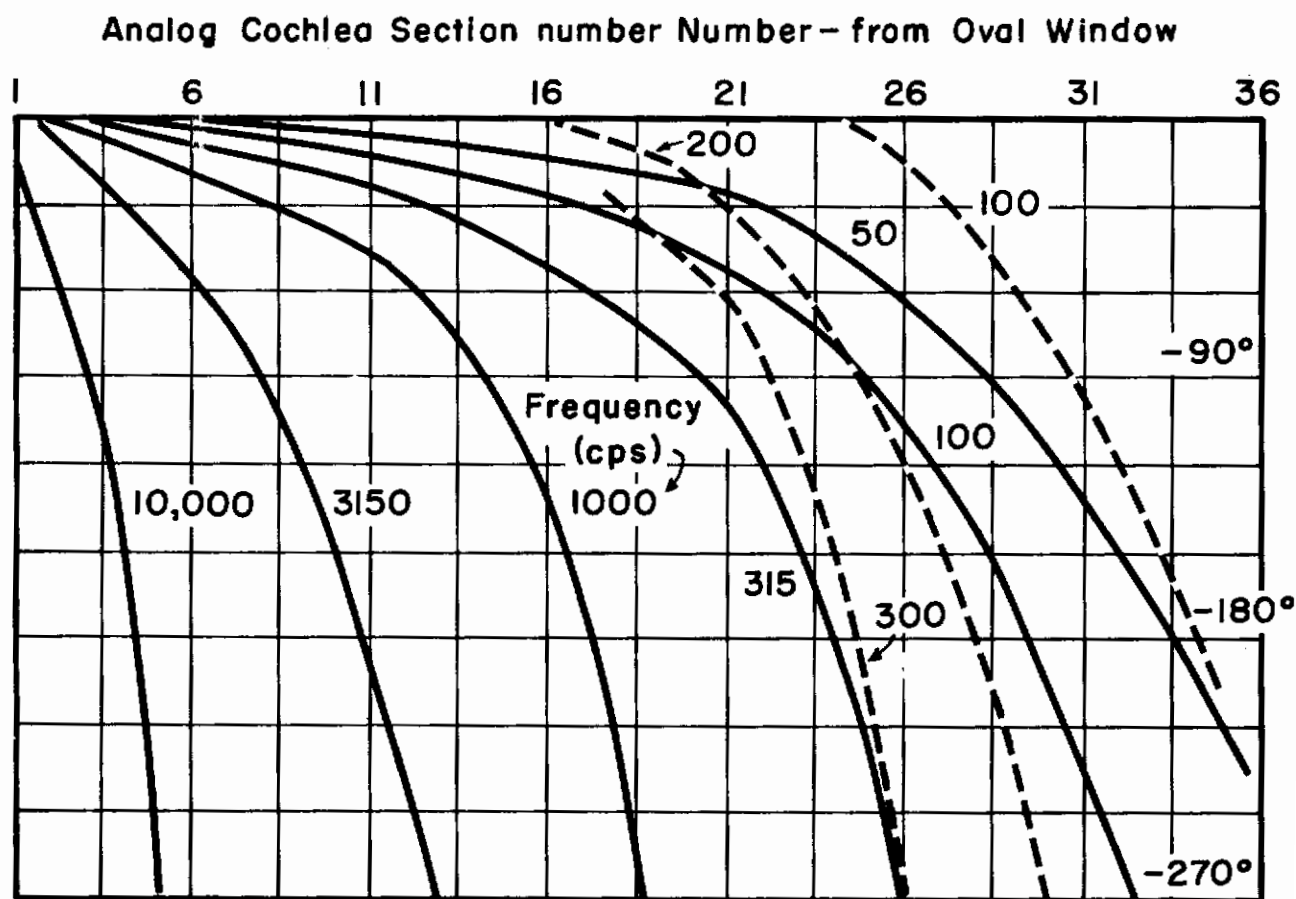
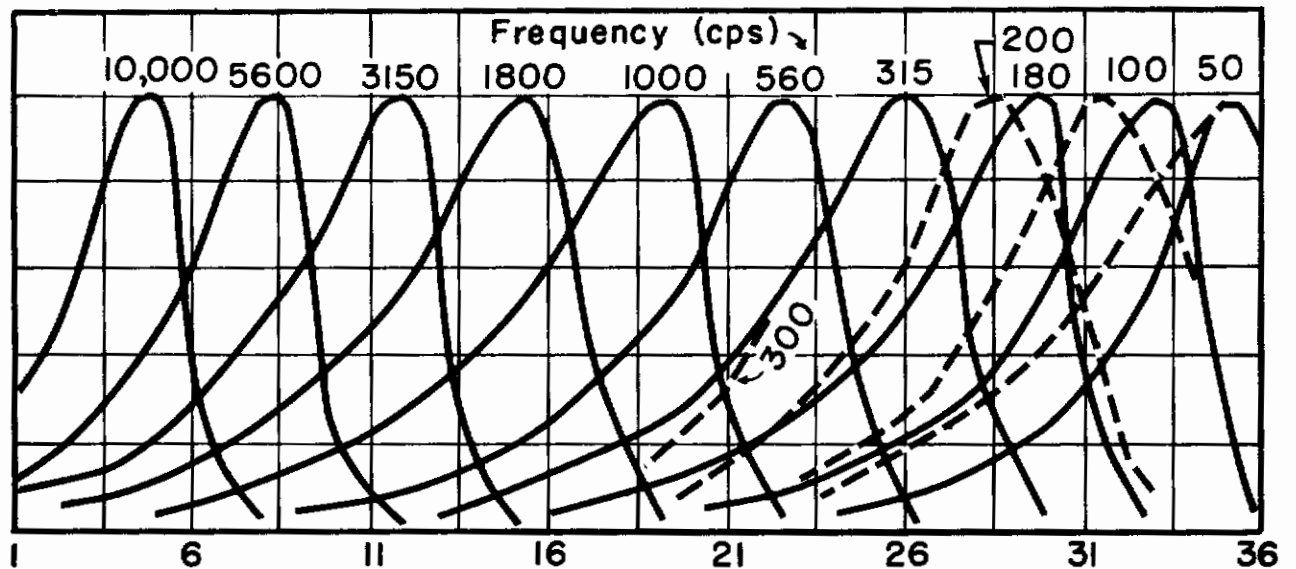


Figure 24. Circuit for Simulation of the Cochlea Input Impedance



The top shows velocity and displacement magnitude,
the bottom figure shows displacement phase

————— Analog cochlea data

----- Human cochlea data

Figure 25. Magnitude and Phase of Basilar Membrane Motion

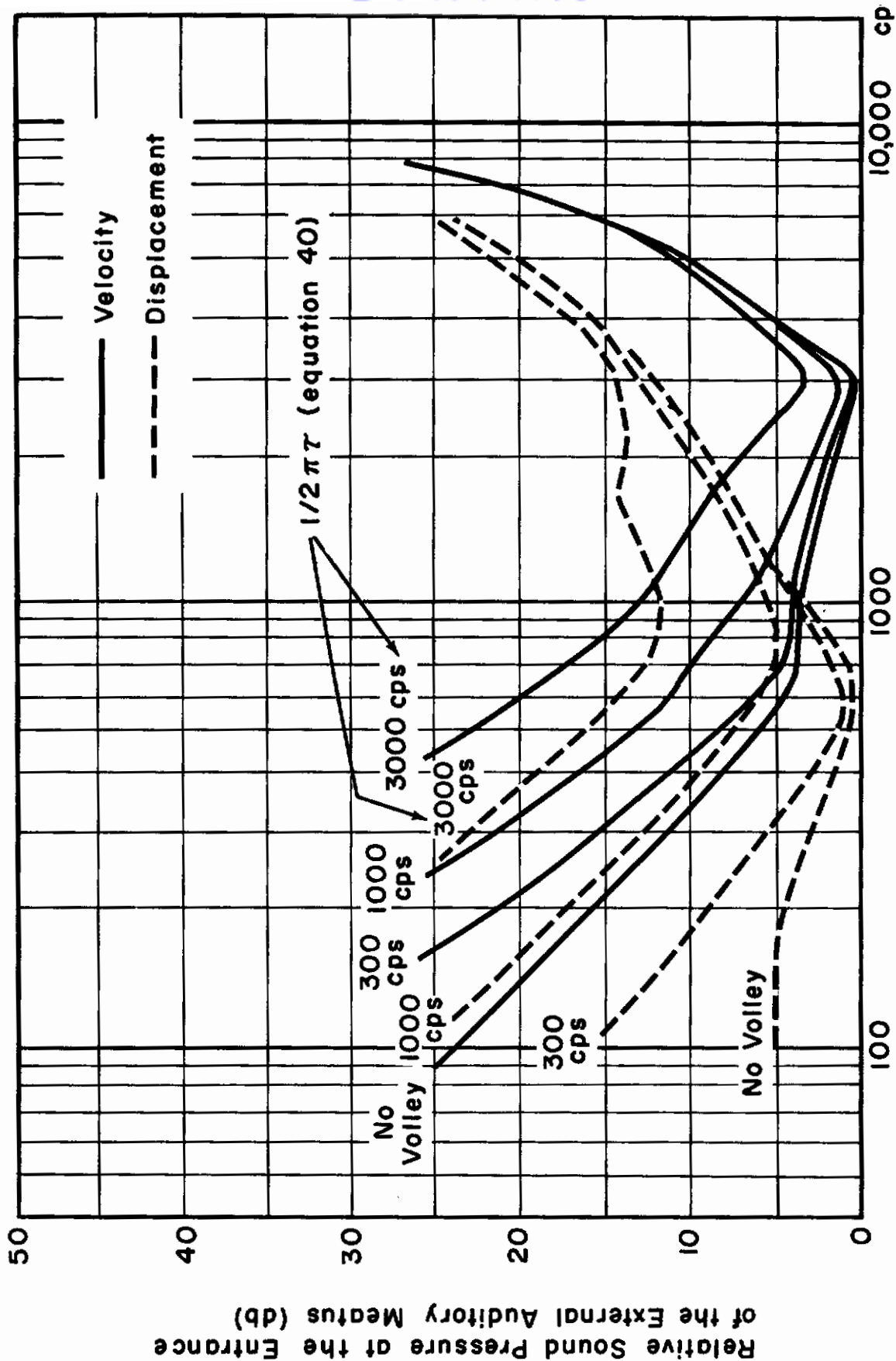


Figure 26. Analog Threshold Curves for Velocity and Displacement

as the important characteristic of motion when frequency $1/2\pi\tau$ is 1000 cps. The resulting threshold of hearing curve for the analog is compared to several human threshold curves in figure 27 (ref. 24).

Sustained Sound Recognition

Theoretical studies preceding the development of the model for sound recognition were based on a pattern theory (ref. 10). Subsequent theoretical and experimental studies were made of cochlear pattern recognition, and experimental results of analog recognition were compared with human recognition to determine their degree of correspondence (ref. 8). The monopolar and quasi-continuous patterns from the analog ear may be described by a function $f(x) \geq 0$, where $f(x \leq 0) = f(x \geq L) = 0$, and L is the length along which the sensory structures are distributed in the cochlea. A mathematical function is used to recognize the pattern produced by the Electronic Analog Ear. Of the several functions proposed for recognition, only the results of the cross-correlation analysis will be considered here.*

Define $f(x)$ as an unknown pattern to be recognized. Define $g_i(x)$ as the i^{th} pattern from a dictionary of M patterns. Recognition results when one of the $g_i(x)$ is selected as a representation of the unknown pattern $f(x)$. The recognition process is to select that $g_i(x)$ that corresponds to a maximum of the function

$$\frac{\int_0^L f(x) g_i(x) dx}{\sqrt{\int_0^L f^2(x) dx \int_0^L g_i^2(x) dx}} \quad (84)$$

Normalization of the recognition function may be accomplished by making the energy of the $g_i(x)$ equal, and hence recognition may be made independent of the amplitude of the unknown pattern. The recognition process implies minimum mean-square error (ref. 8).

The stimulus material used in the study consisted of eight vowels, each vowel both voiced and whispered, recorded on tape by a trained speaker. The vowels (*i, I, e, æ, a, ʌ, u*) were used as presentations to human subjects, from which recognition/confusion matrices were determined, and as inputs to the Electronic Analog Ear, from which they were photographed. The data from the photographs was used to obtain the correlation matrices of voiced and whispered vowels. A scatter diagram of the combination of cross correlation and the recognition/confusion matrices is shown in figure 28. The indication is that analog and human recognition processes show

* Recent theoretical studies have generated criteria for animal perception as constrained by neural noise and matters of environment. Results of this theory show modified (nonlinear) cross correlation to be optimum. Changes in the idealized correlation function are necessitated by the fact that neural noise is strongly stimulus dependent. In addition, neural noise is distinctly nonwhite.

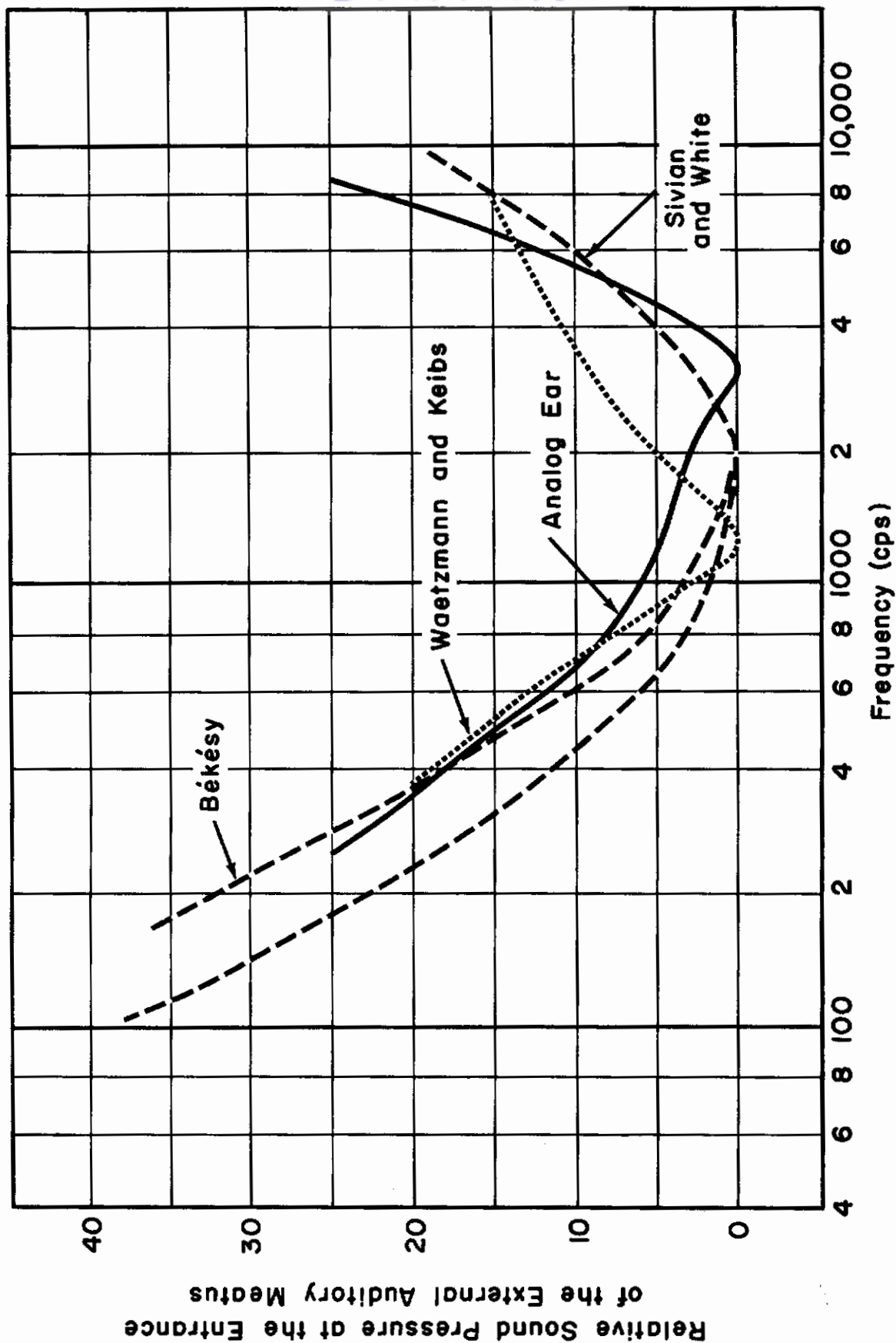
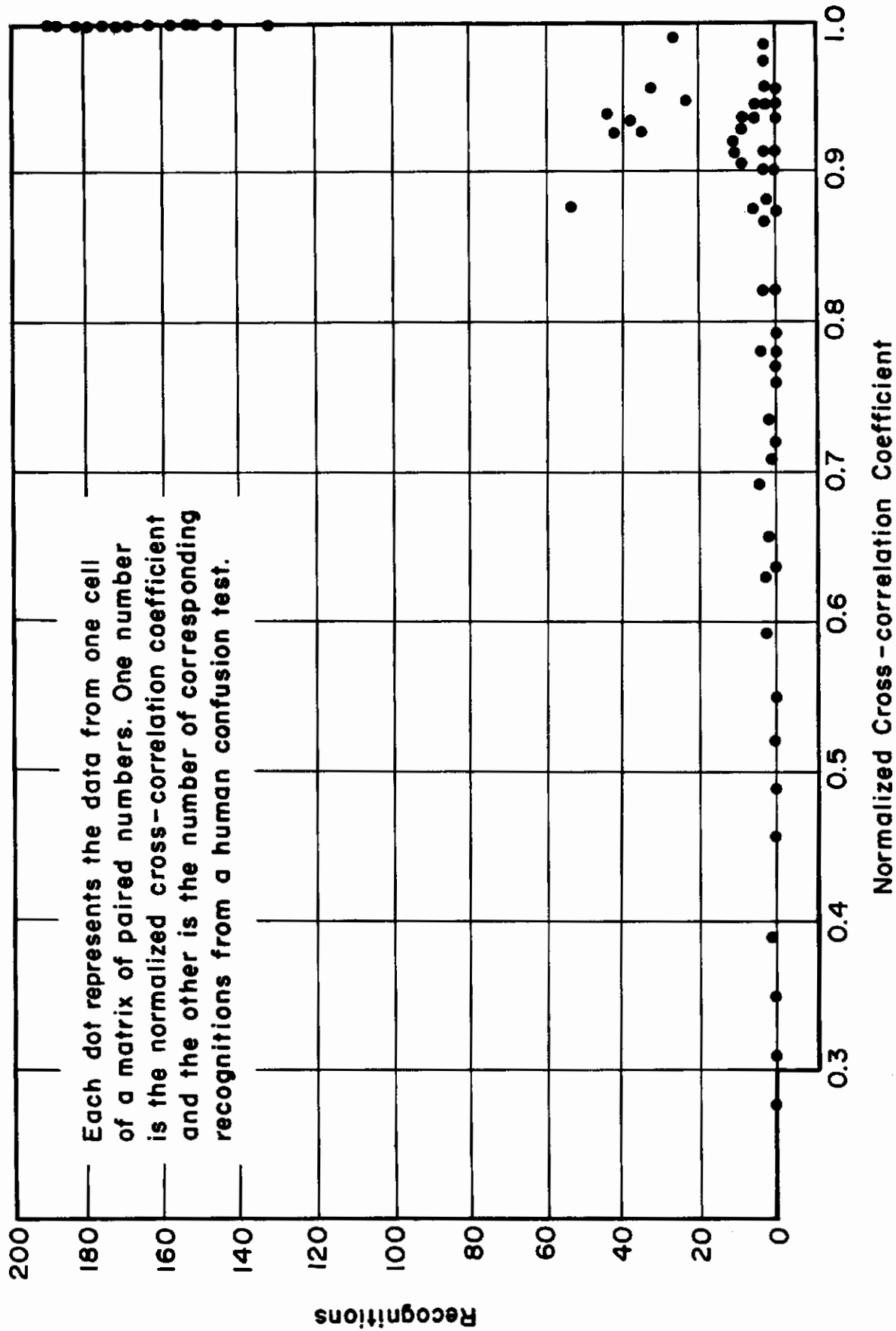


Figure 27. Comparison of Auditory Thresholds



similarities.* Also of interest is the result that there is little difference in the pattern or recognition of voiced and whispered vowels.

SUMMARY

The results of this research are broad. It was originally proposed that an analog of the ear be developed and built. This was done. It has been shown that this analog models the hearing system in certain respects. There are many things about the ear that are not modeled. Some are important and bear on general transfer sound-to-pattern characteristics, such as mutual inhibition and phasic-tonic neural behavior. Others, such as the middle ear reflexes and fatigue, may be of only second-order importance for speech recognition. The model which has been proposed and has been built as an analog is an abstraction of those parameters of the ear which were considered to be important at the outset of the investigation or whose importance was subsequently recognized.

The process of modeling requires a constant comparison of the model and the measured real world. It must be kept in mind in any research endeavor that knowledge of the real world is limited by the ability to make measurements. In the case of the human ear, measurements are extremely difficult to make; the introduction of an analog which can be compared to a physiological specimen or used to demonstrate psychoacoustic phenomena can make some experiments much more simple and can aid in the interpretation of others.

The present analog is one of the first such complete models of the ear (first patterns in 1961), and while it has shown important similarities to the human ear, it is not yet complete or finished. Subsequent studies and modifications are necessary which will cause the analog to more closely approach a complete simulation.

* That analog and human processes are similar is perhaps best demonstrated from recent results in which analog ear patterns were matched so as to produce intelligible synthetic speech obtainable by means of narrow-band waveform data.

A GRAPHICAL CALCULUS OF APPROXIMATION
WITH APPLICATION TO AN ANALOG FOR THE EARIntroduction

Concern here is for the structure of a lumped parameter, linear, passive, bilateral network representation for a system which can be explained in terms of a set of partial differential equations. Consideration is limited to those systems which show mutual and self terms of the sort $ax + bdx/dt + c\int xdt$; higher-order derivatives and integrals than the first will not be considered.

The calculus to be developed is of a graphical nature such that neither the original partial differential equations nor the network ordinary differential equations need be known explicitly. A physical network will be deduced whose element values must be found in terms of appropriate boundary conditions (i.e., from the pertinent physics of the system). The development requires knowledge of the relationships between a network and its describing equations.

The generalized calculus will be exemplified for two important physiological systems. First will be described the mammalian cochlea, or inner ear, for which the conventional first-order transmission line representation will be derived. In addition, the second-order approximation will be indicated, in which it becomes evident that the classical incrementalization of the structure into Δx lengths is no longer possible. Application of the second-order representation to the tympanic membrane (eardrum) reveals a provocative general technique for broadbanding.

It is emphasized that techniques to be described are general for the class of systems described at the outset. As such, many portions of living and other systems may be represented in approximation.

The General Method

Select points in the region of interest at which approximations are to be obtained. The density of points implies the nature of the "granularity" or "sampling" error; if too sparse, the approximation will be poor, and if too dense, the approximation will be impractically complex. An actual example of a familiar sort is a segment of an ordinary transmission line which is represented in terms of a sequence of simple lumped-parameter networks. If the number of segments is too small, the cut-off frequency for propagation will be too small in comparison with the unlimited cut-off frequency of the idealized uniform structure; the larger is the number of sections (the denser the points in the approximation), the larger is the cut-off frequency and the smaller is the granularity or sampling error. In a qualitative way, the density of points (which need not be uniform) should be chosen according to the structural detail of the physical system which is to be approximated. Let a voltage v_i exist at each point P_i . Voltage v_i is measured with respect to a single reference or ground point. The variable v_i represents a plausible analogous physical variable, such as velocity. Let v_i be influenced by operator $a + bd/dt + c\int/dt$ concerning itself with similar operators for every other variable v_j for $j \neq i$. A

generalized circuit representation is thus obtained as a three-dimensional network which is symbolized in figure 29 in terms of self and mutual parallel resonant circuits. Mutual inductance and capacitance elements in this circuit may be negative or positive.

Voltage in the network of figure 29 is analogous to some other variable depending upon the problem of interest, such as field potential, velocity, force, chemical concentration, etc. The analogous quantity need not always be the voltage v_i in figure 29 measured with respect to a single reference node; variables of importance may be a set of node voltage differences such that no single reference node is evidenced.

In addition to the nodal system of figure 29, there also exist networks described by loop currents in which analogous variables consist of suitable branch currents. In the case of loops, individual branch impedances are series resonant circuits instead of parallel resonant circuits as in figure 29. In certain simple cases, the loop system may be derived as the dual of the nodal system. However, existence of a dual is not assured when mutual inductance occurs and/or when the network is not planar. In any event, two representations (one nodal and one loop) can always be found, where the two may or may not be duals.

In any given network, two variables, voltage and current, are of importance. For the analogous system, there may (or may not) also be two variables; in the case of hydrodynamics, for example, the two are pressure and fluid velocity which relate in terms of a mechanical impedance. In the electric network, the ratio of voltage to current is impedance and special input and transfer impedances may be important measures; note, however, that if only voltages v_i in figure 29 are of interest, for example, such impedances are of little direct concern.

A given electric network will have analogous variables which are node pair voltages or branch currents; many choices for these exist in determining the network. In some cases, convenient identification of both current and voltage with, say, pressure and velocity, may not be possible, whereas in others, it may. If, for example, input impedance to an hydraulic system is also to be represented in electric network form, it is evidently necessary that both voltages and currents be identified with equivalent hydraulic variables. On the other hand, if only biochemical enzyme concentration is of concern, only analogous voltage or only analogous current need be considered.

The Cochlea

The inner ear consists of a fluid-filled channel separated over most of its length by an elastic membranous duct (the cochlear duct) which has properties of mass, viscous friction, and elastance. A representation is shown in figure 30.

Select for this system a set of points arrayed along the cochlear duct. Voltages at the circuit analog points can represent some component of duct velocity (transverse, longitudinal, etc.). The first task of representation is selection of suitable points. An array along the duct is appropriate if interest is primarily in the motion of the duct. Note

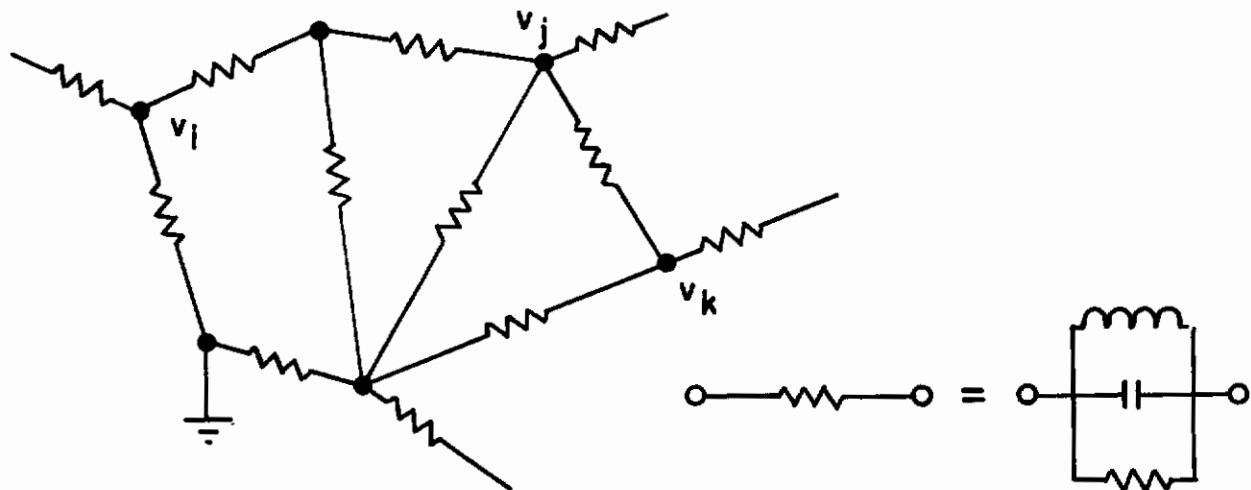


Figure 29. The Generalized Nodal System

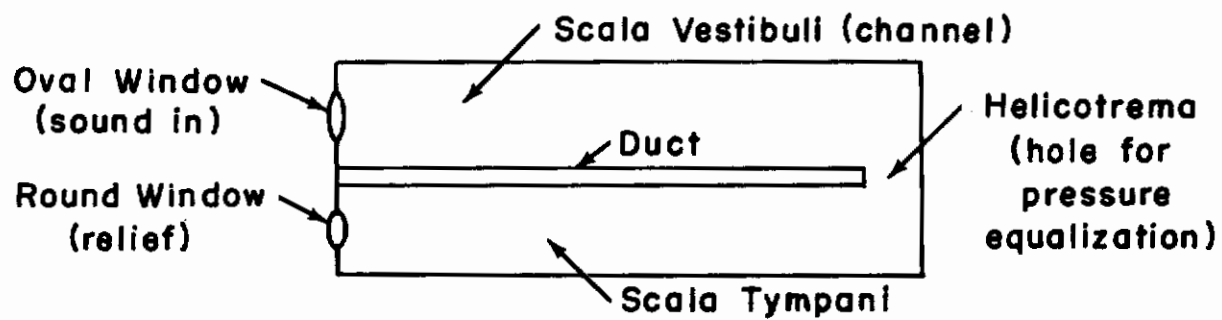


Figure 30. Simplified Diagram of the Cochlea

especially that this assumption leaves unanswered the detailed description of the scalae (except as reflected in actual element values of the circuit representation) although it yields the most accurate possible description of duct motion for a given number of points.

The second task is the designation of what voltage v_1 signifies. It is believed the neural activity depends on transverse motion of the duct, and transverse velocity may be taken as the representation. Note that axial velocity or a mixture could be chosen with no change in the generalized circuit configuration other than element values after employing boundary value data.

The circuit that results for the cochlea is shown in figure 31 where, for clarity, existence of mutual elements is implied with arrows. Observe that figure 31 is a quite general circuit; it is nothing more than the circuit of figure 29 drawn slightly differently. The fact that it is supposed to represent a cochlea is not yet explicit.

The simplest possible approximation relevant to figure 31, which again does not apply explicitly to any given structure, ignores all mutual terms other than first-order ones. The result is a ladder network consisting of pi sections where each branch is a parallel resonant circuit. This simple system has a dual which is a ladder network consisting of tee sections where each branch is a series resonant circuit. The resonant arm nonuniform ladder is thus potentially a very general first-order approximation to a distributed system in which the approximation is achieved by ignoring most of the mutual elements.

The first-order network has, as stated, branches which are parallel resonant circuits. A consideration of boundary values (i.e., the tendency of the human cochlea to act as a sequence of low-pass circuits) implies that the series arm has no capacitance; the result is figure 32. Increments of lengths Δx for the cochlea may be identified with individual tee sections; boundary values may thus be applied on a section-by-section basis so as to evaluate parameters.

The rather "crude" approximation of figure 32, remembering that scalae are given little consideration in the selection of points, makes it evident that parameters will not show direct correspondence with comparable parameters of the actual cochlea. An inductance represents a fictional "equivalent" elasticity, capacitance and "equivalent" mass, and so forth. Improved correspondence between physical and network parameters is achieved only through use of higher-order network approximations in which spatial points of approximation are assumed to lie in the scalae as well as in the cochlear duct.

It should be observed in figure 32 that a tapering of element values so as to account for "end effect" near the helicotrema is not inconsistent with the general approximation.

The dual of figure 32 is shown in figure 33. This circuit is also a practical one in which velocity may be acquired as an unbalanced voltage if each series branch coil is realized as the primary of a transformer. Note that figure 33 also obtains directly from the generalized loop system such that the nodal system need not be derived first.

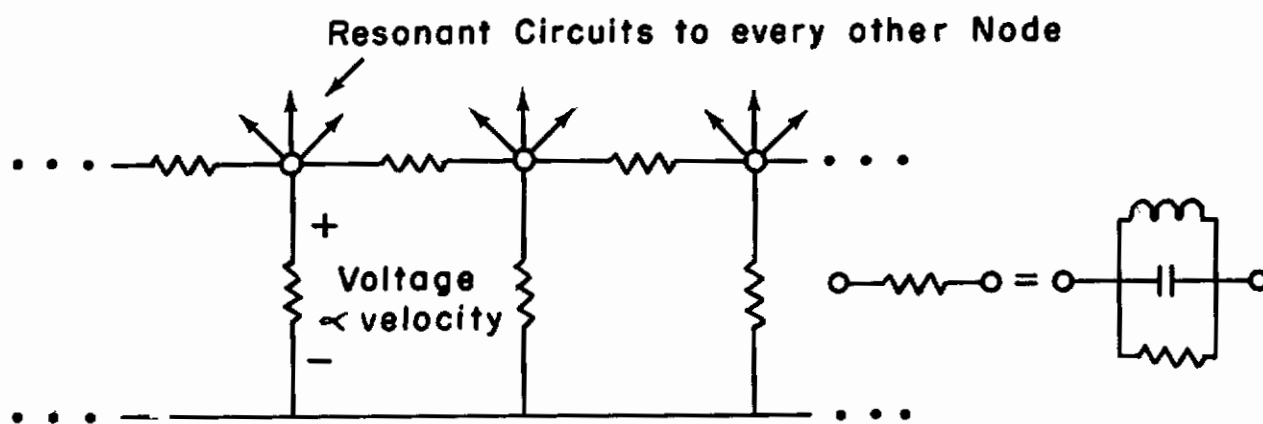


Figure 3| Generalized System for Velocity

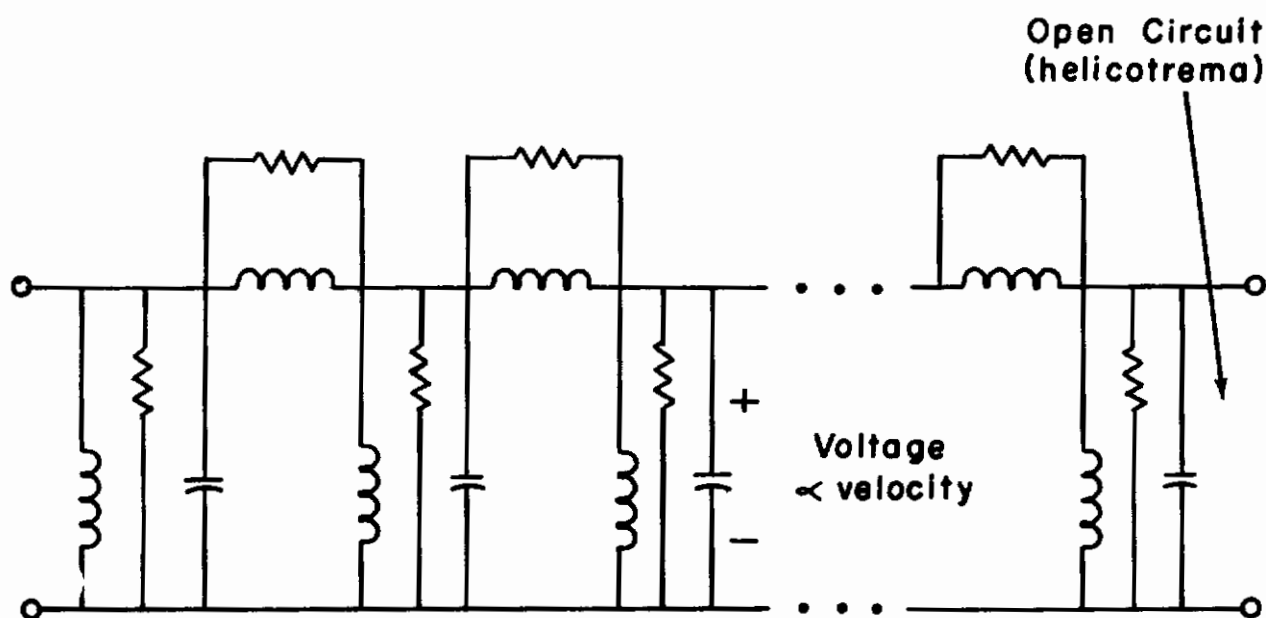


Figure 32. The First Order Equivalent for the Cochlea

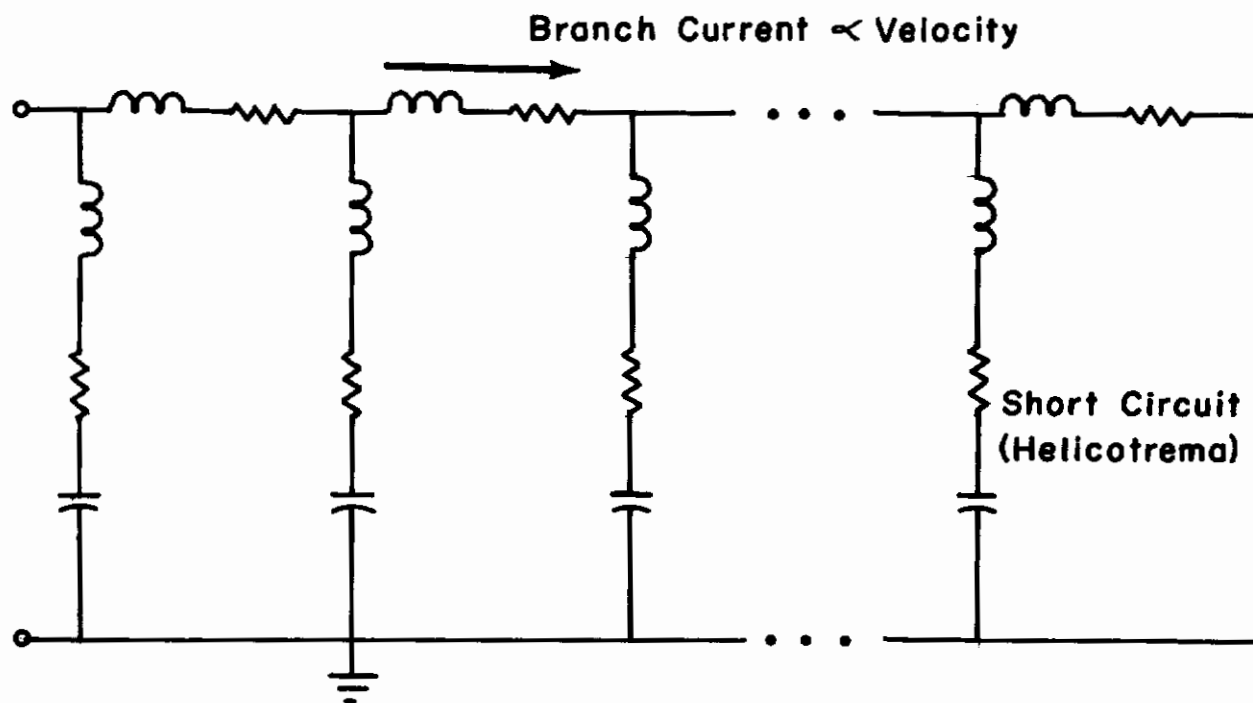


Figure 33. The First Order Loop Equivalent

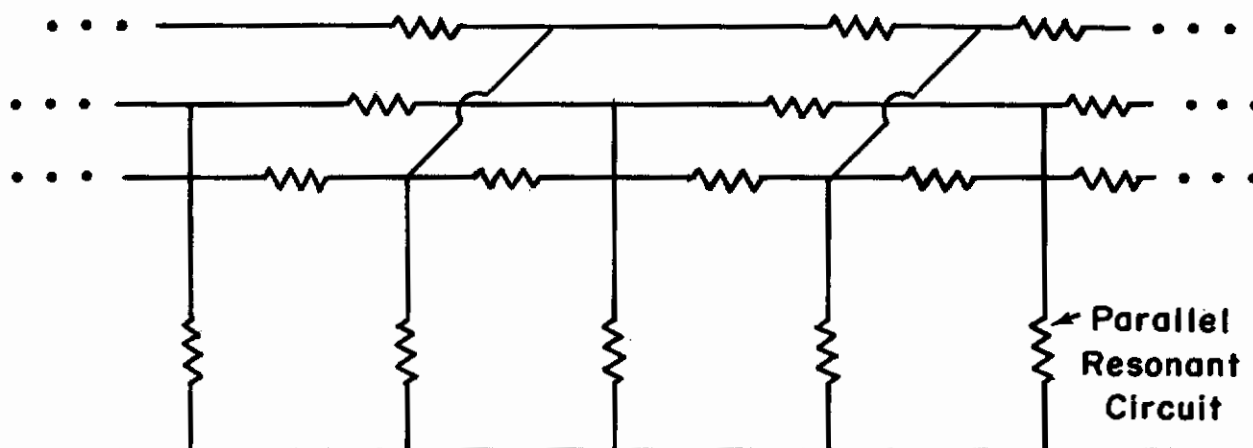


Figure 34. The Second Order Nodal System

In figure 32, only node voltages have been given direct analog significance (and in figure 33, only loop currents). Although transverse velocities of points along the basilar membrane are represented in figures 32 and 33, pressure differences are not. Pressure difference for figure 32 is the current in the shunt branch, which constitutes the self-admittance. Identification of an input or transfer impedance applicable to the entire network is not readily demonstrable; a different selection for analogous analog parameters can modify this situation, as will be discussed in the sequel.

It will be self-evident to the networks specialist that foregoing networks, which are unbalanced, may be balanced or quasi-balanced in a variety of ways. In this manner, an animal cochlea with its two scalae of either equal or differing dimensions may be more closely represented than with an unbalanced structure.

Cochlear Second-Order Approximation

It is of interest to consider inclusion of the first- and second-order mutual terms but not those of higher order. As before, assume all points are in the cochlear duct to give the circuit of figure 34. Although the network is not greatly complicated structurally, it is far more cumbersome when it comes to the determination of element values. This is because the circuit can no longer be incrementalized in a physically revealing manner such that boundary conditions can be applied to individual increments. Continuously bridged systems of this sort, especially when extremely nonuniform as in the mammalian cochlea, are not solved by known techniques in network analysis.

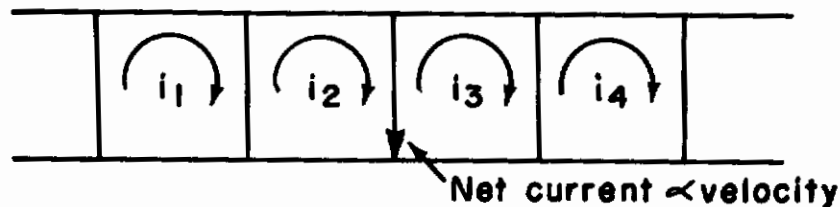
Another Cochlea Convention

The series of points in figure 31 provide voltages which are presumed to represent transverse velocities of points along the basilar membrane. As stated previously, designation of the meaning of v_i is somewhat arbitrary. Equivalent circuits for the basilar membrane as have appeared in the literature are not the same as those shown thus far in this discussion. These different equivalents were obtained by others from a direct first-order analysis of the hydrodynamic equations for the cochlea. It may be presumed that the meaning associated with v_i differs from that employed thus far; in fact, it is not necessarily implied that various investigators used points of representation which are uniformly displaced along the cochlear duct.

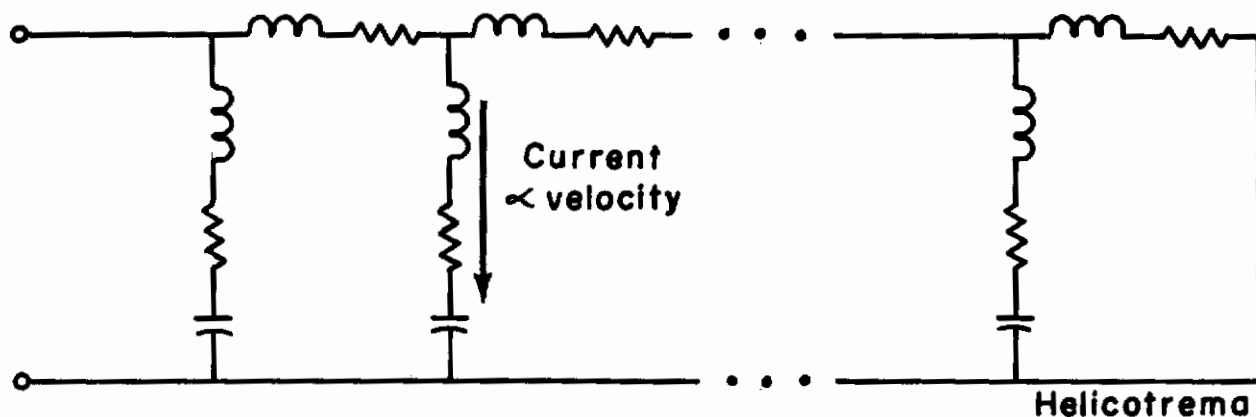
Analysis of points selection and equivalent circuits given elsewhere show the following: A loop-type, first-order analysis is made instead of a nodal type. The difference in adjacent loop currents is presumed to be transverse velocity; the specific currents are those in the shunt branches rather than in the series branches of the network as in figure 33. Figure 35a shows the proper interpretation. The equivalent, allowing for a boundary property, is shown in figure 35b, and the dual in figure 35c. The dual may be obtained directly from a nodal analysis by assuming velocity relates to the voltage differences between adjacent loops in figure 32.

The network of figure 35b is the one most cited in the literature. It provides the advantage of representing both pressure and velocity such

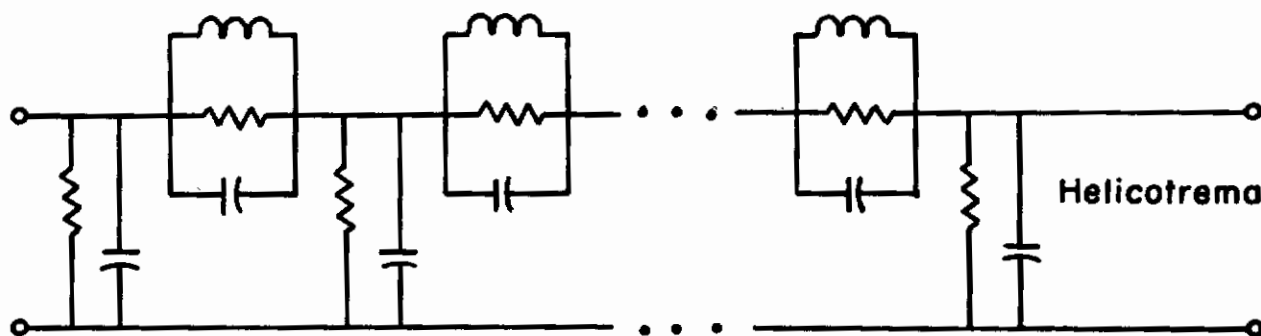
Contrails



(a)



(b)



(c)

Figure 35. Equivalent Cochlea Based on Loop Current or Node Voltage Differences

that electrical input impedance of figure 35b is related to mechanical input impedance of the actual cochlea. Clearly, results here imply that many different equivalent circuits exist depending on certain arbitrary definitions and assumptions. Some of these, such as in figure 35a, provide a closer analog for a gross impedance than do others. Some, such as figure 31, provide more direct generalization to relatively high orders of approximation.

The Tympanic Membrane

The membrane is separated into two distinct regions, one which is stiffened by attachment to the malleus (one of the three middle ear bones, or ossicles), and a more freely moving part. The two parts are mutually coupled in two different and opposing ways. First, the fibers of one part of the membrane exercise direct force on the other part. Second, the limited air cavity of the middle ear exercises elastic coupling from one part to the other.

An appropriate equivalent circuit uses two points of approximation and a reference point. Let voltage be velocity and current be pressure. Two current sources occur, both applied from the outer ear (in phase), one for each part of the membrane. The equivalent circuit is shown in figure 36a. In the dual of figure 36b, the two voltages are proportional, since voltage is pressure in the outer ear (times area) which is presumed to be uniform over the cross-section of the external auditory meatus (ear canal). In order to show a single voltage source, we may employ the artifice of the ideal transformer with the result of figure 36c. The transformer may be adjusted, as a rule, to achieve physical realization of the circuit when negative elements exist in the mutual branch in figure 36b. Note in figure 36c that, by moving the load along its series circuit so as to have it next to the primary of the transformer, it becomes possible to define an unbalanced system such that both source and load have a common ground.

A study of the tympanic membrane shows that separation into three regions is logical. One part is associated with the malleus as before. The free portion of the membrane has two distinct parts, one of which is relatively flexible. The loop equivalent is shown in figure 37. It is of interest to observe how the three generators in figure 37 aid one another in causing current to flow into the load. The three generators provide proportional voltages and hence may be obtained from a single voltage source using ideal transformers.

An elementary analysis of figure 36c reveals how broadbanding is accomplished. Assume a circuit in which the only loss is represented by the (resistive) load. The transfer function is found to have two pairs of complex conjugate poles in the left-half plane and a pair of conjugate zeros on the $j\omega$ axis (plus one at the origin). Except for the conjugate zeros, the transfer function is capable of representing a broadband band-pass circuit. Actual broadbanding may be realized by moving the j -axis zeros to the interior of the left half plane. This can be achieved by adding loss in either or both of the resonant circuits not associated with the load. The broadbanding principle thus appears to be one in which lossy, coupled resonant circuits are employed. Analysis carried out elsewhere shows that the pass-band characteristic in human hearing is due mostly to the middle ear. In view of its physical size, the ear is a fairly good transducer for matching air and fluid media.

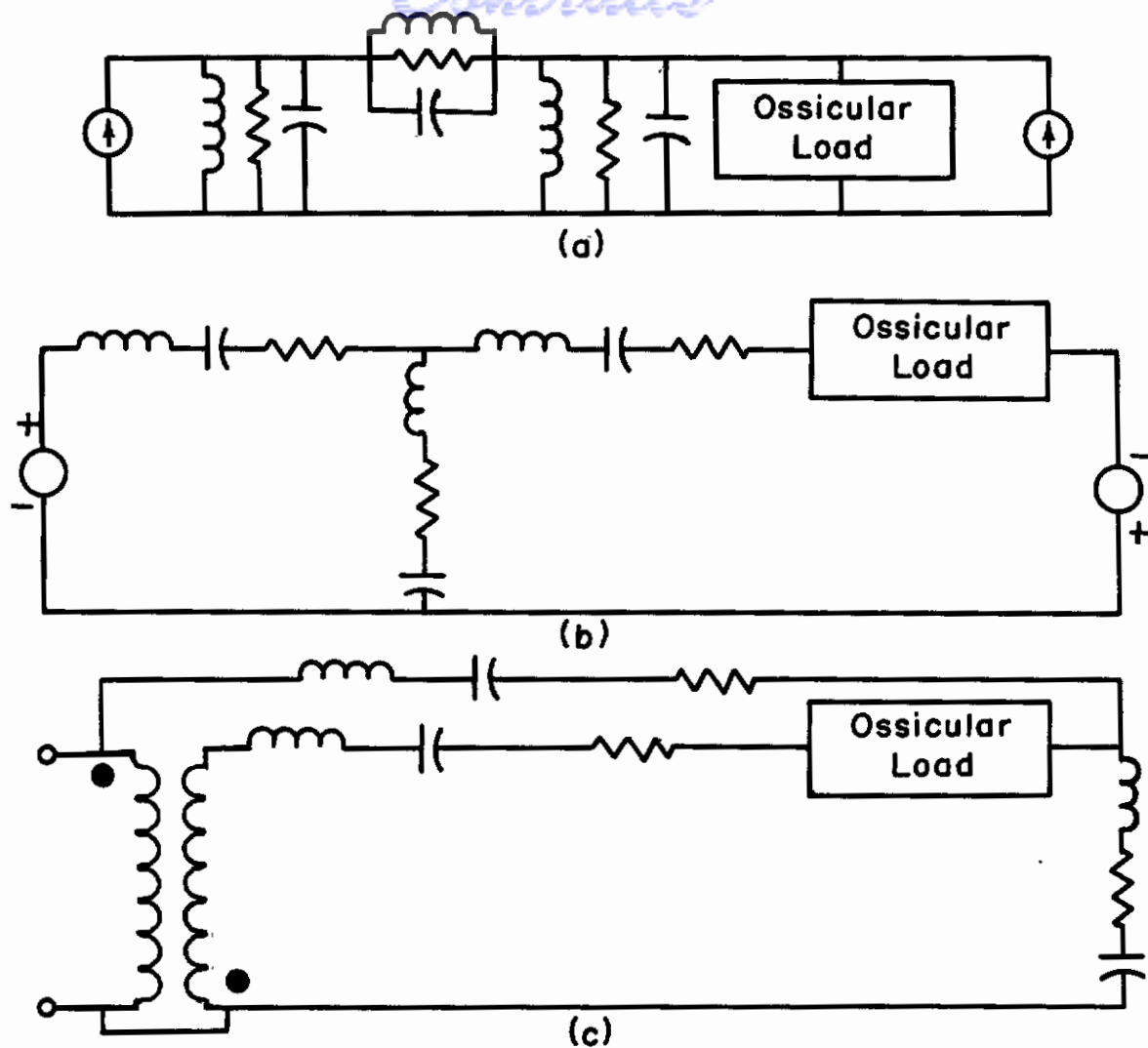


Figure 36. Approximations for the Tympanic Membrane

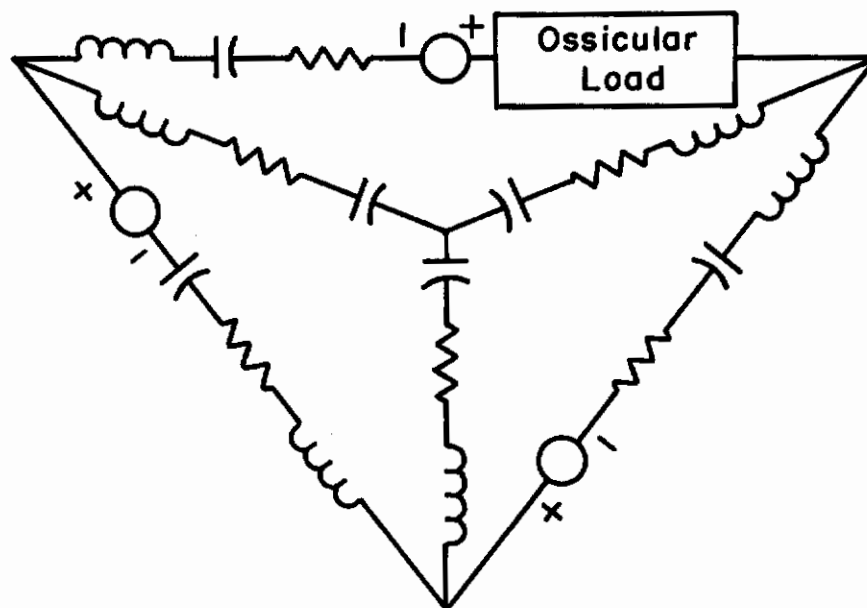


Figure 37. The Second Order Approximation for the Tympanic Membrane

REFERENCES

1. von Békésy, G., Experiments in Hearing, McGraw-Hill Book Co., Inc., New York, 1960.
2. Zwislocki, J., "Theorie der Schneckenmechanik," Acta Oto-Laryngologica, Suppl. 72, 1948.
3. Peterson, L. C. and Bogert, B. P., "A Dynamical Theory of the Cochlea," J. Acoust. Soc. Amer., 22 (1950), pp 369-381.
4. Fletcher, H., "On the Dynamics of the Cochlea," J. Acoust. Soc. Amer., 23 (1951), pp 637-645.
5. Bauch, H., "Die Schwingungsform der Basilarmembran bei Erregung durch Impulse und Gerausche, gemessen an einem elektrischen Modell des Innenohres," Frequenz, 10 (1956), pp 222-234.
6. Wansdronk, C., On the Mechanism of Hearing, Philips Research Laboratories, Eindhoven, Netherlands, 1961.
7. Caldwell, W. F., Glaesser, E., and Stewart, J. L., "Design of an Analog Ear," in E. E. Bernard and M. R. Kare (Eds.) Biological Prototypes and Synthetic Systems, Plenum Press, New York, 1962.
8. Caldwell, W. F., The Analysis of Complex Sounds by Cochlear Patterns, Doctoral dissertation, University of Arizona, 1962.
9. Glaesser, E., An Analog of the Ear, Doctoral dissertation, University of Arizona, 1962.
10. Stewart, J. L., "A Model for Hearing," in E. E. Bernard and M. R. Kare (Eds.) Biological Prototypes and Synthetic Systems, Plenum Press, New York, 1962.
11. Stewart, J. L., "Quantitative Laws for Sensory Perception," Psych. Rev., Vol. 70, pp 180-192, March, 1963.
12. Stewart, J. L., "A Law for Loudness Discrimination," Science, Vol. 137, pp 618-619, 24 August, 1962.
13. Wever, E. G., Theory of Hearing, John Wiley and Sons, Inc., New York, 1949.
14. Zwislocki, J., "Theory of Temporal Auditory Summation," J. Acoust. Soc. Amer., 32 (1960), pp 1046-1060.
15. Zwislocki, J., "Some Impedance Measurements on Normal and Pathological Ears," J. Acoust. Soc. Amer., 29 (1957), pp 1312-1317.
16. Moller, A. R., "Network Model of the Middle Ear," J. Acoust. Soc. Amer., 33 (1961), pp 168-176.
17. Onchi, Y., "A Study of the Mechanism of the Middle Ear," J. Acoust. Soc. Amer., 21 (1949), pp 404-410.

Contrails

18. Onchi, Y., "Mechanism of the Middle Ear," J. Acoust. Soc. Amer., 33 (1961), pp 794-805.
19. Wansdronk, C., On the Mechanism of Hearing, Philips Research Laboratories, Eindhoven, Netherlands, 1961.
20. Wiener, F. M., and D. A. Ross, "The Pressure Distribution in the Auditory Canal in a Progressive Sound Field," J. Acoust. Soc. Amer., 18 (1946), pp 401-408.
21. von Békésy, G. and W. A. Rosenblith, "The Mechanical Properties of the Ear," Handbook of Experimental Psychology (Ed. by S. S. Stevens), John Wiley and Sons, Inc., New York, 1951, pp 1075-1115.
22. Covell, W. P., "The Ossicles in Otosclerosis," Acta Oto-Laryngologica, vol XXVII, 1940, pp 264-276.
23. Fletcher, H., "The Dynamics of the Middle Ear and Its Relation to the Acuity of Hearing," J. Acoust. Soc. Amer., 24 (1952), pp 129-131.
24. Licklider, J. C. R., "Basic Correlates of the Auditory Stimulus," Handbook of Experimental Psychology (Ed. by S. S. Stevens), John Wiley and Sons, Inc., New York, 1951, pp 985-1039.